EI 32

UDC 621.313.322:538.24:62–56

ACTA POLYTECHNICA SCANDINAVICA

ELECTRICAL ENGINEERING SERIES No. 32

Utilization of harmonics for self-excitation of a synchronous generator by placing an auxiliary winding in the rotor

TAPANI JOKINEN

Helsinki University of Technology, Otaniemi, Finland

Thesis for the degree of Doctor of Technology to be presented with due permission for public examination and criticism in the Auditorium S 4 at the Helsinki University of Technology (Otaniemi, Finland) on the 20th of October, 1973, at 12 o'clock noon.

HELSINKI 1973

ABSTRACT

This study is concerned with a new excitation system in which a voltage is induced by the flux density harmonics of the air-gap in an auxiliary rotor winding supplying the field winding through a rectifier. The system is brushless and self-regulated. The applicability of various harmonics for producing the excitation current is studied; it has been shown that the field current component proportional to the resulting air-gap flux can only be obtained by means of permeance variations due to irregularities of the stator air-gap face. The field current component proportional to the load current can be produced by harmonics due to the stator winding distribution. Experimental studies were made with a generator of 3 kVA size, in which the first slot harmonic was utilized to create the excitation current. The generator has characteristics similar to those of conventional compounded synchronous generators. The measurements show that the method presented for calculating the terminal voltage gives a satisfactory result in practice.

CONTENTS

Page

BASIC SYMBOLS 7
1 INTRODUCTION 11
2 SELF-REGULATION 12
3 HARMONICS OF FLUX DENSITY IN THE AIR-GAP OF AN ALTERNATING-CURRENT MACHINE 14
3.1 Flux density distribution in the general case 14
3.2 Flux density distribution in a constant air-gap 17
3.2.1 M.m.f. of an alternating-current winding 17
3.2.1.1 Double-layer windings 17
3.2.1.2 Single-layer windings 23
3.2.2 Slot harmonics 25
3.3 Harmonics of flux density distribution due to the permeance variations . . . 26
3.3.1 Harmonics due to rotor eccentricity 26
3.3.2 Harmonics due to saturation 29
3.3.3 Harmonics due to salient-pole rotor 30
3.3.4 Harmonics due to slot openings 30
3.3.4.1 Slotted stator 30
3.3.4.2 Slotted rotor 35
3.3.4.3 Slotted stator and rotor 36
3.3.5 Harmonics due to shaped stator air-gap face 36
3.4 Applicability of harmonics in producing excitation voltage 38
4 RECTIFICATION 41
4.1 Equivalent rating 41
4.2 *m*-phase rectification 42
4.3 Replacing the rectifier load by an equivalent resistance load 44
5 AUXILIARY WINDING OF THE ROTOR 46
5.1 Equivalent circuit for the auxiliary winding 46
5.2 Build-up of self-excitation 47
5.3 Field current supplied by the auxiliary winding 48
5.4 Design considerations 51
6 LOAD CHARACTERISTICS 55
6.1 Field current 55
6.2 Voltage equations of a synchronous generator 58
6.3 Direct-axis magnetizing reactance 59
6.4 Terminal voltage 59
6.5 Effect of speed change on the terminal voltage 62
7 PARALLEL OPERATION 65
8 EXPERIMENTAL INVESTIGATIONS 67
8.1 Experimental generator 67

8.2 Circuit elements 69
8.2.1 Resistances 69
8.2.2 Reactances 69
8.2.3 Factor C_1 72
8.2.4 Factor C_2 73
8.3 Terminal voltage 74
8.3.1 Terminal voltage as a function of load current 74
8.3.2 Terminal voltage as a function of speed 77
8.3.3 Sudden load change 77
8.3.4 Terminal voltage waveform 78
9 CONCLUSIONS 79
ACKNOWLEDGEMENTS 80
REFERENCES 81

BASIC SYMBOLS

Lower case symbols are used for the instantaneous values of electrical quantities; upper case symbols are used for their r.m.s. and average values; upper case boldface symbols are used for phasors; lower case symbols with ^ are used for peak values.

Subscripts

A auxiliary winding of rotor
F field winding
p fundamental
λ permeance harmonic having λ pole pairs
μ permeance harmonic having μ pole pairs
ν harmonic due to winding distribution having ν pole pairs
1 stator
2 rotor

Symbols

A	area
A_j	copper area of one conductor
a	linear current density; number of parallel paths
b	flux density
$b_{k(p+gQ1)}$	flux density harmonic due to stator winding distribution having $p + gQ_1$ pole pairs
$b_{u(p+gQ1)}$	flux density harmonic due to stator slot openings having $p + gQ_1$ pole pairs
b_I, b_{II}, b_{III}, b_{IV}	flux density harmonic groups (Eqs. (7)···(10))
C	integration constant; capacitance
C_k	capacitance (Boucherot)
C_1	abbreviation (Eq. (108))
C_2	abbreviation (Eq. (111))
c	integer
D	air-gap diameter
f_m	magnetomotive force
G	field current/air-gap voltage (Eq. (122))
g	integer
h	magnetic field strength
I	current
I_a	active current

I_{Ak}	short-circuit current of auxiliary winding
I_r	reactive current
I_t	direct current
I_u	field current component proportional to stator terminal voltage
I_v	phase current
I_{v1}	fundamental component of phase current
$I_{x\sigma}$	field current component proportional to voltage drop in stator leakage reactance
I_ϕ	field current component proportional to resulting air-gap flux
I'	field current component proportional to stator current
I_{1d}	direct-axis component of stator current
$\bar{i}$	dimensionless fraction (Eq. (98))
K	equivalent rating of auxiliary winding/d.c. power
K	integer
K_I	compound factor
K_t	direct current/fundamental phase current for rectifier circuit
K_1	abbreviation (Eq. (72))
K_2	constant
k	variable (Eq. (97))
k	integer
k_c	Carter's coefficient
k_k	saturation factor
k_1, k_2	integers
L	effective core length
$\bar{l}$	ratio of reactive powers of two generators in parallel connection
l_{Am}	mean length of one turn of the auxiliary winding
m	number of phases
N	denominator of number of slots per pole per phase reduced to lowest terms
N_t	number of turns of a winding in series
N_u	number of conductors in one slot
n	frequency of rotation
n	order of harmonic; integer
P	active power
p	number of pole pairs
$\bar{p}$	ratio of active powers of two generators in parallel connection
Q	number of slots; reactive power
Q_a	number of open slots; reactive power of generator (a)
q	number of slots per pole per phase
R	resistance

R'	equivalent resistance of rectifier load per phase
r	air-gap radius
s	slip
T	numerator of number of slots per pole per phase reduced to lowest terms
t	time; tooth pitch
U	voltage; terminal voltage (to neutral)
U_{Af}	synchronous voltage of auxiliary winding
U_{Afk}	component of U_{Af} proportional to stator current
U_{Afu}	component of U_{Af} proportional to fundamental of flux density wave
U_{A1}	abbreviation (Eq. (95))
U_f	synchronous voltage
U_i	air-gap voltage
U_t	arithmetic mean of direct voltage
U_v	phase voltage
U_o	voltage acting on rectifier bridge below the threshold voltage
v	magnetic potential difference
v_{z2}	magnetic potential difference over rotor tooth (rotor-tooth m.m.f.)
v_δ	magnetic potential difference over air-gap (air-gap m.m.f.)
X	reactance
X_{A1}	abbreviation (Eq. (96))
X_m	magnetizing reactance
X_{md}	direct-axis magnetizing reactance
X_{mq}	quadrature-axis magnetizing reactance
X_σ	leakage reactance
x_4	length of slot opening
y, y_1, y_2	coil pitch
Z	load impedance
Z_F	impedance defined by Eq. (104)
Z_L	load impedance containing the stator resistance and leakage reactance
β	function (Eq. (64))
β_ν	angle between reference axis and positive crest value of the νth harmonic (Fig. 4)
γ	electrical conductivity
δ	air-gap length
δ_i	phase difference of $\mathbf{U}_f$ with respect to $\mathbf{U}_i$
δ''	equivalent air-gap
δ''_ν	equivalent air-gap for the νth harmonic
δ_o	mean air-gap length

ϵ	eccentricity of rotor
ϑ	angular coordinate
Λ	permeance per unit area (specific permeance)
Λ_{kQ1}	specific permeance having kQ_1 pole pairs
Λ_o	mean value of specific permeance
λ	number of pole pairs of permeance harmonic
μ	number of pole pairs of permeance harmonic; reduction factor
μ_o	permeability of free space
ν	number of pole pairs of harmonic due to winding distribution
ξ	winding factor
ξ_{p+gQ1}	winding factor of stator winding for the harmonic having $p + gQ_1$ pole pairs
$\xi_{\epsilon\nu}$	slot opening factor for the νth harmonic
σ	leakage coefficient
τ	pole pitch; function (Eq. (64))
φ	impedance angle of load
φ_F	phase difference of $\mathbf{I}_\phi$ with respect to $\mathbf{U}_1$
φ_L	impedance angle of load containing the stator resistance and leakage reactance
φ_ϵ	phase angle of permeance harmonic due to eccentricity
φ_ν	phase angle of the νth harmonic due to winding distribution
φ_λ, φ_μ	phase angle of the λth and μth permeance harmonic, respectively
ω	angular frequency
ω_ϵ	angular frequency of permeance harmonic due to eccentricity

1 INTRODUCTION

The magnetic flux density in the air-gap of an alternating-current machine contains a large number of harmonics in addition to the fundamental determined by the pole pair number of the machine. These harmonics are usually objectionable. They cause supplementary losses, harmonics in the waveform of a generator's voltage, parasitic torques; they create noise; etc. In [1], [15] and [21] a method has been presented by which the third harmonic of flux density can be utilized for the excitation of a synchronous machine. The method involves furnishing an auxiliary winding in the stator, having a pole pair number three times the fundamental pole pair number. The voltage induced by the third harmonic in this auxiliary winding is rectified and supplied over slip rings to the field winding. Measurements have shown that the voltage induced in the auxiliary winding increases, with increasing load current of the machine, approximately as the field current required to compensate the armature reaction. This is true within a fairly wide power factor range; less perfectly with leading than lagging power factor. The system is not self-regulating, however, and it needs an excitation control. It has been proven that fast voltage control is possible by this method in transient states.

PLATTHAUS [17] demonstrated in his thesis that no special auxiliary winding is needed: the voltage induced by the third harmonic in the armature winding may be utilized as excitation voltage by providing an appropriate circuit.

In accordance with a suggestion made by Professor T. Pyökäri, those possibilities shall be studied here which exist for utilizing the flux density harmonics to create the excitation voltage by placing an auxiliary winding in the rotor; the type of characteristics attainable in a generator excited in this way shall also be considered. In the study of harmonics a particular search shall be made for those whose magnitude changes, with a change of load, similarly as the field current required for a constant terminal voltage. If such harmonics are found and if they are strong enough, a self-regulating synchronous generator, requiring no slip rings or brush gear can be devised. In cases where high reliability and low maintenance are desired a brushless generator is the best solution, because the brush gear is the component causing the greatest need of maintenance and most of the faults. In hazardous atmospheres no slip rings can be used owing to risk of explosion due to sparking, unless the machine is pressurized or has a flame-proof enclosure. Such expensive designs are avoidable by using a brushless generator.

2 SELF-REGULATION

When the load of a synchronous generator changes and there is no regulation of excitation, the terminal voltage of the generator changes due to the armature reaction and due to change of the voltage drops across the leakage reactance and the resistance of the stator winding. In order to maintain a constant terminal voltage the field current must be regulated. One means of regulating the field current is to use a so-called *compound scheme.* A great number of different compound circuits is known [24]. These can be divided into two principal groups: current addition circuits, and voltage addition circuits.

The phasor diagram of a non-salient-pole generator is seen in Fig. 1. The stator resistance is assumed to be negligible. $\mathbf{U}_1$, $\mathbf{U}_i$ and $\mathbf{U}_f$ are the terminal voltage, air-gap voltage and synchronous voltage, respectively. $\mathbf{I}_1 jX_m$ and $\mathbf{I}_1 jX_{1\sigma}$ are the voltage drops in the stator magnetizing reactance X_m and in the leakage reactance $X_{1\sigma}$. The field current $\mathbf{I}_F$ can be divided into two components, $\mathbf{I}_\phi$ and $\mathbf{I}'$. I_ϕ produces the resulting flux and is proportional to U_i. I' compensates the armature reaction and is proportional to the load current I_1. $\mathbf{I}_\phi$ can further be divided into two components $\mathbf{I}_u$ and $\mathbf{I}_{x\sigma}$ (Fig. 1).

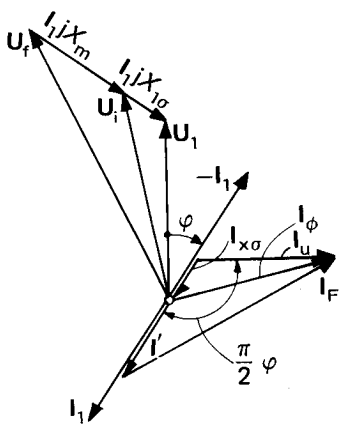

Fig. 1. The phasor diagram of a non-salient-pole generator.

$\mathbf{I}_u$ is proportional to the terminal voltage and lags it by 90°, while $\mathbf{I}_{x\sigma}$ is proportional to the voltage drop $I_1 X_{1\sigma}$ and is in phase with the load current. Hence the field current is

$$\mathbf{I}_F = \mathbf{I}_u - \mathbf{I}_{x\sigma} - \mathbf{I}' \tag{1}$$

The phase difference of $\mathbf{I}_u$ with respect to $\mathbf{I}_{x\sigma} + \mathbf{I}'$ is $\frac{\pi}{2} + \varphi$, where φ is the impedance angle of the load. Good voltage control should comply with Equation (1) so that I_u remains constant when the load current varies.

The principle circuit diagram Fig. 2 shows a compound circuit where the field current components are added. The current $\mathbf{I}_D$ of a reactor D lags the terminal voltage $\mathbf{U}_1$ by 90°. Thus the component I_u of the field current can be composed of I_D. The component proportional to the load current is constituted by the secondary current of the current transformer M. The phase difference of $\mathbf{I}_D$ with respect to $\mathbf{I}_M$ is the required $\frac{\pi}{2} + \varphi$. When the sum of $\mathbf{I}_D$ and $\mathbf{I}_M$ is rectified, a field current I_F is obtained.

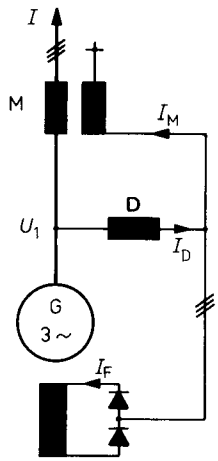

Fig. 2. A current addition compound circuit.

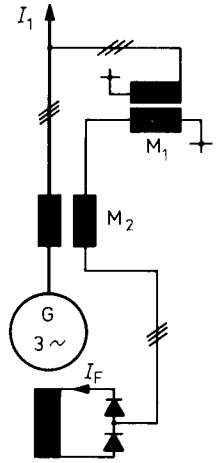

Fig. 3. A voltage addition compound circuit.

Another compound circuit i.e., the voltage addition circuit, is shown in Fig. 3. Here, the required angle $\frac{\pi}{2} + \varphi$ is present between the secondary voltages of the voltage transformer M_1 and the current transformer M_2. By vectorial addition of the voltages the necessary excitation voltage and field current are obtained. The compound circuits of Figs. 2 and 3 are said to be *negatively compounded.*

If the terminals of the secondary winding of the current transformer in Figs. 2 and 3 are reversed, the phase of the field current component proportional to the load current changes 180°. A compound machine connected in this manner is said to be *positively compounded* and it has a constant power factor independent of the load when connected to infinite busbars [5]. Positive compounding is applied in synchronous motors.

3 HARMONICS OF FLUX DENSITY IN THE AIR-GAP OF AN ALTERNATING-CURRENT MACHINE

Harmonics of the flux density in the air-gap arise from two causes:

1. The winding is discontinuous. It is concentrated in slots and coil groups. Hence the air-gap m.m.f. (the magnetic potential difference over the air-gap) produced by the winding is not sinusoidal.

2. The permeance of the air-gap is not constant. Permeance variations are caused by the stator and rotor slot openings, salient poles, magnetic saturation, and rotor eccentricity.

In the next chapter we discuss the harmonics of the flux density distribution produced by the air-gap m.m.f. and air-gap permeance in the general case. Subsequently, we study the harmonics of the flux density distribution created by a distributed winding when the air-gap permeance is constant, and finally we consider the flux density harmonics due to the permeance variations mentioned under 2 above.

The winding is assumed to be symmetric, implying that its phase windings are identical and uniformly distributed in space. The phase currents flowing in the stator windings are assumed to be balanced and sinusoidal.

Regarding the fractional-slot windings the following assumptions are made:

1. There are always $2m$ phase spreads per pole pair, m being the number of phases;
2. There are only two kinds of phase spread, having slot numbers per pole per phase (q_a and q_b) differing by 1: $q_a = q_b + 1$.

By combining these phase spreads in various manners, we obtain the desired number of slots per pole per phase. For instance, if the denominator of the number of slots/pole/phase reduced to its lowest terms is five, there are three possible combinations for accomplishing the winding:

1. $q_a\ q_b\ q_b\ q_b\ q_b$
2. $q_a\ q_b\ q_a\ q_b\ q_b$
3. $q_a\ q_a\ q_b\ q_b\ q_b$

In practice, the conditions specified above are nearly always satisfied.

3.1 FLUX DENSITY DISTRIBUTION IN THE GENERAL CASE

When considering the air-gap flux density distribution, the current flowing in a winding may be replaced by a linear current density. The linear current density is a periodic function of time and space and can be described by a series

$$a = -\sum_{\nu} \hat{a}_\nu \sin(\nu\vartheta - \omega_\nu t - \varphi_\nu) \tag{2}$$

where ν is the number of pole pairs and $\hat{a}_\nu$ the amplitude of the harmonic linear current density, ω_ν the angular frequency, φ_ν the time phase difference with respect to the reference chosen and ϑ the angular coordinate.

A linear current density distribution produces a m.m.f. in a closed magnetic circuit. In the following the air-gap is considered to be enlarged to the degree that its permeance is half of the permeance of the entire magnetic circuit. The magnetic potential difference over this equivalent air-gap is an integral of the linear current density distribution [20, p. 128]:

$$v = r \int a \, \mathrm{d}\vartheta = r \sum_\nu \frac{\hat{a}_\nu}{\nu} \cos(\nu\vartheta - \omega_\nu t - \varphi_\nu) + C \tag{3}$$

where C is the integration constant and r the radius of the air-gap. The ratio of the air-gap flux density to the air-gap m.m.f., i.e. the permeance per unit area, is called in this paper *the specific permeance of the air-gap*. The specific permeance of a constant air-gap (δ) is

$$\Lambda = \frac{\mu_0}{\delta} \tag{4}$$

The specific permeance in rotating machines is a periodic function of time and space. It is therefore expressible as a series

$$\Lambda = \Lambda_0 + \sum_\mu \hat{\Lambda}_\mu \cos(\mu\vartheta - \omega_\mu t - \varphi_\mu) \tag{5}$$

where μ is number of pole pairs of the harmonic permeance, Λ_0 the mean value of the specific permeance and $\hat{\Lambda}_\mu$ the amplitude of the μth harmonic.

The flux density is the product of the air-gap m.m.f. and the air-gap specific permeance:

$$\begin{aligned}
b = v\Lambda = &\left[r\sum_\nu \frac{\hat{a}_\nu}{\nu}\cos(\nu\vartheta - \omega_\nu t - \varphi_\nu) + C\right]\left[\Lambda_0 + \sum_\mu \hat{\Lambda}_\mu \cos(\mu\vartheta - \omega_\mu t - \varphi_\mu)\right] = \\
&= r\Lambda_0 \sum_\nu \frac{\hat{a}_\nu}{\nu}\cos(\nu\vartheta - \omega_\nu t - \varphi_\nu) + C\Lambda_0 + \\
&\quad + r\sum_\nu \frac{\hat{a}_\nu}{\nu}\cos(\nu\vartheta - \omega_\nu t - \varphi_\nu)\sum_\mu \hat{\Lambda}_\mu \cos(\mu\vartheta - \omega_\mu t - \varphi_\mu) + \\
&\quad + C\sum_\mu \hat{\Lambda}_\mu \cos(\mu\vartheta - \omega_\mu t - \varphi_\mu) \\
&= r\Lambda_0 \sum_\nu \frac{\hat{a}_\nu}{\nu}\cos(\nu\vartheta - \omega_\nu t - \varphi_\nu) + \qquad \text{(1st term)} \\
&\quad + C\Lambda_0 + \qquad \text{(2nd term)} \\
&\quad + r\sum_\nu \sum_{\substack{\mu \\ \nu \neq \pm\mu}} \frac{\hat{a}_\nu \hat{\Lambda}_\mu}{2\nu}\cos[(\nu \pm \mu)\vartheta - (\omega_\nu \pm \omega_\mu)t - (\varphi_\nu \pm \varphi_\mu)] + \qquad \text{(3rd term)} \\
&\quad + r\sum_\mu \frac{\hat{a}_{\pm\mu}\hat{\Lambda}_\mu}{\pm 2\mu}\cos[\pm 2\mu\vartheta - (\omega_{\nu=\pm\mu} \pm \omega_\mu)t - (\varphi_{\nu=\pm\mu} \pm \varphi_\mu)] + \qquad \text{(4th term)} \\
&\quad + r\sum_\mu \frac{\hat{a}_{\pm\mu}\hat{\Lambda}_\mu}{\pm 2\mu}\cos[(\omega_{\nu=\pm\mu} \mp \omega_\mu)t + (\varphi_{\nu=\pm\mu} \mp \varphi_\mu)] + \qquad \text{(5th term)} \\
&\quad + C\sum_\mu \hat{\Lambda}_\mu \cos(\mu\vartheta - \omega_\mu t - \varphi_\mu) \qquad \text{(6th term)}
\end{aligned} \tag{6}$$

Since the νth harmonic of the linear current density and the μth harmonic of the permeance are due to different causes, ω_ν is not necessarily equal to ω_μ, nor is φ_ν necessarily equal to φ_μ even though ν and μ are equal. For this reason at certain points in the preceding expression the subscript $\nu = \pm\mu$ has been written for ω_ν and φ_ν. In each expression the upper signs are simultaneously valid, or the lower signs.

Assuming that no unipolar flux exists in the machine, the integration constant C is determined in accordance with the condition that the mean value of the flux density over the air-gap periphery is zero:

$$\int_0^{2\pi} b\,\mathrm{d}\vartheta = 0$$

Carrying out the quadrature and resolving for C yields

$$C = -\frac{r}{\Lambda_0}\sum_{\mu}\frac{\hat{a}_{\pm\mu}\hat{\Lambda}_\mu}{\pm 2\mu}\cos\left[(\omega_{\nu=\pm\mu} \mp \omega_\mu)t + (\varphi_{\nu=\pm\mu} \mp \varphi_\mu)\right]$$

Substitution of C in (6) causes the 2nd and 5th terms to vanish. The air-gap flux density distribution is therefore a sum of the following four harmonic groups:

$$b_{\mathrm{I}} = r\Lambda_0\sum_{\nu}\frac{\hat{a}_\nu}{\nu}\cos(\nu\vartheta - \omega_\nu t - \varphi_\nu) \tag{7}$$

$$b_{\mathrm{II}} = r\sum_{\nu}\sum_{\substack{\mu \\ \nu\neq\pm\mu}}\frac{\hat{a}_\nu\hat{\Lambda}_\mu}{2\nu}\cos\left[(\nu \pm \mu)\vartheta - (\omega_\nu \pm \omega_\mu)t - (\varphi_\nu \pm \varphi_\mu)\right] \tag{8}$$

$$b_{\mathrm{III}} = r\sum_{\substack{\mu \\ (\nu=\pm\mu)}}\frac{\hat{a}_{\pm\mu}\hat{\Lambda}_\mu}{\pm 2\mu}\cos\left[\pm 2\mu\vartheta - (\omega_{\nu=\pm\mu} \pm \omega_\mu)t - (\varphi_{\nu=\pm\mu} \pm \varphi_\mu)\right] \tag{9}$$

$$\begin{aligned} b_{\mathrm{IV}} = -\frac{r}{\Lambda_0}\sum_{\lambda}\sum_{\substack{\mu \\ (\nu=\pm\mu)}}\frac{\hat{a}_{\pm\mu}\hat{\Lambda}_\mu\hat{\Lambda}_\lambda}{\pm 4\mu}\Big\{&\cos\Big[\lambda\vartheta - [\omega_\lambda + (\omega_{\nu=\pm\mu} \mp \omega_\mu)]t + \\ &- [\varphi_\lambda + (\varphi_{\nu=\pm\mu} \mp \varphi_\mu)]\Big] + \cos\Big[\lambda\vartheta - [\omega_\lambda - (\omega_{\nu=\pm\mu} \mp \omega_\mu)]t + \\ &- [\varphi_\lambda - (\varphi_{\nu=\pm\mu} \mp \varphi_\mu)]\Big]\Big\} \end{aligned} \tag{10}$$

Of the double signs, the upper ones are simultaneously valid, or the lower ones. In (9) and (10) μ obtains only those values of ν for which $\nu = \pm\mu$. The second subscript λ of the specific permeance in (10) assumes all those values for which there exist permeance waves.

First, the flux density distribution comprises the same harmonics (b_{I}) as the linear current density distribution. In the following, these are termed *harmonics due to the stator winding distribution.* Secondly, the linear current density and the permeance harmonics in combination produce a large number of harmonics (b_{II}, b_{III}, b_{IV}) with different numbers of pole pairs and different angular frequencies. These shall be called *harmonics due to the permeance variations.*

Starting from the same initial condition, namely that there is no unipolar flux, FROHNE [8, p. 131 ··· 134] has arrived at a conclusion partly at variance with the above-stated. In addition to the harmonics (7)···(10) he found one further harmonic group, which is unipolar. This clearly contradicts the initial condition stated above.

3.2 FLUX DENSITY DISTRIBUTION IN A CONSTANT AIR-GAP

The mean value Λ_0 of the specific permeance function (5) states the specific permeance of the equivalent air-gap (δ''_ν):

$$\Lambda_o = \frac{\mu_0}{\delta''_\nu}$$

The equivalent air-gap is a function of the pole-pair number of the m.m.f. wave; it has therefore the subscript ν. The equivalent air-gap can be calculated from the equation

$$\delta''_\nu = k_c k_k \delta \tag{11}$$

where δ is the actual air-gap. The coefficient k_c takes into account the slot openings and the coefficient k_k, the saturation. The coefficient k_c is often called Carter's coefficient; it can be calculated by a method presented in [19, p. 177]. The saturation factor k_k can be calculated from the equation

$$k_k = \frac{f_{m\nu}}{2\nu_{\nu\delta}}$$

where $f_{m\nu}$ is the total m.m.f. of the νth harmonic and $\nu_{\nu\delta}$ the part thereof acting on one air-gap.

The νth harmonic of the air-gap m.m.f. produces a harmonic flux density

$$b_\nu = \Lambda_o \nu_\nu = \frac{\mu_0}{\delta''_\nu} \nu_\nu$$

The flux density contains same harmonics as the m.m.f. These harmonics due to the stator winding distribution are proportional to the stator current. It is therefore possible to use these harmonics to produce the field current component proportional to the load current, which is required for self-regulation.

3.2.1 M.m.f. of an alternating-current winding

3.2.1.1 Double-layer windings

A symmetrical double-layer winding as has been defined at the beginning of Chapter 3, may only produce harmonics in accordance with the equation [23, p. 82]

$$\frac{\nu}{p} = \pm \frac{1}{N}(2mg + 2) \quad \text{for even N} \tag{12}$$

$$\frac{\nu}{p} = \pm \frac{1}{N}(2mg + 1) \quad \text{for odd N} \tag{13}$$

$$g = 0, \pm 1, \pm 2, \ldots$$

where m is the number of phases and N the denominator of the number of slots per pole per phase, reduced to its lowest terms,

$$q = \frac{T}{N}$$

The double signs in Eqs. (12) and (13) are chosen to be + or − to make the equations yield the positive sign for the fundamental ($\nu/p = +1$). The ratio of the harmonic pole pairs ν to the fundamental pole pairs p is commonly called the order of the harmonic. In this study the number of harmonic pole pairs ν is also, for simplicity, referred to as the order of the harmonic.

If the coil axis of the first coil in a given coil group is adopted as reference (Fig. 4), the νth m.m.f. harmonic of the entire winding will comply with the equation [23, p. 83]

$$v_\nu = \hat{v}_\nu \cos(\nu\vartheta_1 - \omega t - \varphi + \beta_\nu) \tag{14}$$

φ is the angle shown in the phasor diagram of Fig. 1 in that phase to which the selected first coil belongs, and β_ν is an angle depending on the design of the winding and determined by addition of the individual coils' m.m.f.'s. Eq. (14) is true in coordinates stationary with reference to the stator. When the rotor is rotating at angular velocity ω/p, the following relationship applies between the stator and rotor coordinates ϑ_1 and ϑ_2:

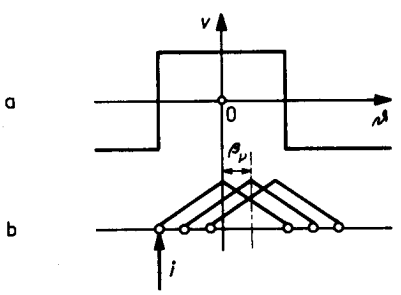

Fig. 4. a) The m.m.f. distribution of one coil. b) The location of the reference axis in the centre of the first coil in a given coil group.

$$\vartheta_2 = \vartheta_1 - \frac{\omega}{p} t + \alpha$$

where α is the angle between the stator and rotor reference axes at $t = 0$. When the time basis is chosen to make the reference axes coincide at the instant $t = 0$, the angle α is zero, and

$$\vartheta_2 = \vartheta_1 - \frac{\omega}{p} t \tag{15}$$

This transformation will be used for conversions from the stator to the rotor coordinates and *vice versa*. Hence, the νth m.m.f. harmonic in the rotor reference frame is

$$v_\nu = \hat{v}_\nu \cos\left[\nu\vartheta_2 - \left(1 - \frac{\nu}{p}\right)\omega t - \varphi + \beta_\nu\right] \tag{16}$$

Assuming the slot to have a negligible width, the m.m.f. distribution is stepped and the amplitude of the νth m.m.f. harmonic is

$$\hat{v}_\nu = \frac{\sqrt{2}}{\pi} \frac{mqN_u}{a} \xi_\nu \frac{p}{\nu} I \tag{17}$$

where I is the r.m.s. phase current, N_u the number of conductors in a slot, a the number of parallel paths and ξ_ν the winding factor. The winding factor and the order ν/p of the harmonic together with their signs have to be substituted in Eq. (17). The current I has a negative value for generator operation and a positive value for motor operation.

In actual truth the slot has a finite width, and there is no abrupt change of the air-gap m.m.f. at the slot; on the contrary, the change occurs gradually across the slot opening, as shown in Fig. 5. In practice, the part ab may be replaced by a straight line, implying analysis of a curve of trapeze shape. The factor by which the coefficients of the Fourier series of the square wave should be reduced in order to find the coefficients of the Fourier series of a trapezoidal wave is [26, p. 31]

$$\xi_{e\nu} = \frac{\sin\left(\frac{\nu}{p} \frac{x_4}{\tau} \frac{\pi}{2}\right)}{\frac{\nu}{p} \frac{x_4}{\tau} \frac{\pi}{2}} \tag{18}$$

where x_4 is the width of the slot opening and τ the pole pitch. This slot opening factor influences the amplitudes of the first slot harmonics and of the higher harmonics. For lower harmonics the coefficient is nearly unity.

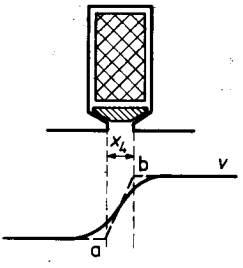

Fig. 5. The change of the air-gap m.m.f. at the slot opening.

Winding factor

In the following, the winding factors and the angle β_ν in Eqs. (14) and (16) are given for different double-layer windings. The equations have been derived in [23, p. 87···97]. The winding factors contain the pitch factor but not the slot-opening factor defined in Eq. (18). The order of a given harmonic ν/p has to be substituted in the equations together with its sign.

Interger-slot winding, N = 1

$$\xi_\nu = \frac{\sin\left(\frac{\nu}{p}\frac{\pi}{2m}\right)}{q\sin\left(\frac{\nu}{p}\frac{\pi}{2mq}\right)} \sin\left(\frac{\nu}{p}\frac{y}{mq}\frac{\pi}{2}\right) \tag{19}$$

$$\beta_\nu = \frac{\pi}{2}\frac{1}{m}\frac{\nu}{p}\left(\frac{1}{q} - 1\right) \tag{20}$$

where y is the coil pitch.

Fractional-slot winding, N = 2

$$\xi_\nu = \frac{\sin\left(\frac{\nu}{p}\frac{\pi}{2m}\right)}{2q\sin\left(\frac{\nu}{p}\frac{\pi}{4mq}\right)} \sin\left(\frac{\nu}{p}\frac{y}{mq}\frac{\pi}{2}\right) \qquad \text{for odd } \nu/p \tag{21}$$

$$\xi_\nu = \pm \frac{\cos\left(\frac{\nu}{p}\frac{\pi}{2m}\right)}{2q\cos\left(\frac{\nu}{p}\frac{\pi}{4mq}\right)} \sin\left(\frac{\nu}{p}\frac{y}{mq}\frac{\pi}{2}\right) \qquad \text{for even } \nu/p \tag{22}$$

$$\beta_\nu = \frac{\pi}{2}\frac{1}{m}\frac{\nu}{p}\left(\frac{1}{q} - 1 \mp \frac{1}{2q}\right) \qquad \text{for any } \nu/p \tag{23}$$

The winding contains phase spreads of two different widths. The upper sign is valid when the reference axis is placed in the centre of the larger phase spread, and the lower sign when it is placed in the centre of the smaller phase spread.

Fractional-slot winding, N = 4

The phase spreads are

$$q_a = q \pm \frac{3}{4}$$

and

$$q_b = q \mp \frac{1}{4}$$

The upper sings are valid for windings with a slots/pole/phase number representable by q = K + 1/4, where K is an integer; the lower signs are valid for windings with q = K − 1/4. An analogous rule is valid for the subsequent equations, too. The sequence of phase spreads is $q_a\ q_b\ q_b\ q_b$. The sequence is valid both for consecutive phase spreads independent of the phase and for consecutive phase spreads in one phase.

If the first coil group defined by the reference axis has q_a slots per pole per phase, the winding factor and the angle β_ν are

$$\xi_\nu = \frac{\sin\left(\frac{\nu}{p}\frac{\pi}{2m}\right)}{4q\sin\left(\frac{\nu}{p}\frac{\pi}{8mq}\right)}\sin\left(\frac{\nu}{p}\frac{y}{mq}\frac{\pi}{2}\right) \qquad \text{for odd } \nu/p \qquad (24)$$

$$\xi_\nu = \pm\frac{\cos\left(\frac{\nu}{p}\frac{\pi}{2m}\right)}{4q\cos\left(\frac{\nu}{p}\frac{\pi}{8mq}\right)}\sin\left(\frac{\nu}{p}\frac{y}{mq}\frac{\pi}{2}\right) \qquad \text{for even } \nu/p \qquad (25)$$

$$\xi_\nu = \frac{\sin\left(\frac{\nu}{p}\frac{\pi}{2m} - \frac{\nu}{p}\frac{\pi}{2}\right)}{4q\sin\left(\frac{\nu}{p}\frac{\pi}{8mq} \mp \frac{\nu}{p}\frac{\pi}{2}\right)}\sin\left(\frac{\nu}{p}\frac{y}{mq}\frac{\pi}{2}\right) \qquad \text{for fractional } \nu/p \qquad (26)$$

$$\beta_\nu = \frac{\pi}{2}\frac{1}{m}\frac{\nu}{p}\left(\frac{1}{q} - 1 \mp \frac{3}{4q}\right) \qquad \text{for any } \nu/p \qquad (27)$$

Fractional-slot winding, N = 5

In this case the windings may be divided into three groups, differing mutually as regards number of slots/pole/phase and sequence of the phase spreads. The slot number per pole per phase in the first coil group is again denoted with q_a.

a) $q = K \pm 1/5$. The phase spreads are

$$q_a = q \pm \frac{4}{5}$$

and

$$q_b = q \mp \frac{1}{5}$$

The sequence of the phase spreads is $q_a\ q_b\ q_b\ q_b\ q_b$. The same order also holds good for phase spreads in one phase.

In this case the winding factor and the angle β_ν can be calculated from the equations

$$\xi_\nu = \frac{\sin\left(\frac{\nu}{p}\frac{\pi}{2m}\right)}{5q\sin\left(\frac{\nu}{p}\frac{\pi}{10mq}\right)}\sin\left(\frac{\nu}{p}\frac{y}{mq}\frac{\pi}{2}\right) \qquad \text{for odd } \nu/p \qquad (28)$$

$$\xi_\nu = \frac{\sin\left(\frac{\nu}{p}\frac{\pi}{2m} - \frac{\nu}{p}\pi\right)}{5q\sin\left(\frac{\nu}{p}\frac{\pi}{10mq} \mp \frac{\nu}{p}\pi\right)}\sin\left(\frac{\nu}{p}\frac{y}{mq}\frac{\pi}{2}\right) \qquad \text{for fractional } \nu/p \qquad (29)$$

$$\beta_\nu = \frac{\pi}{2}\frac{1}{m}\frac{\nu}{p}\left(\frac{1}{q} - 1 \mp \frac{4}{5q}\right) \qquad \text{for any } \nu/p \qquad (30)$$

b) $q = K \pm 2/5$. The phase spreads are

$$q_a = q \pm \frac{3}{5}$$

and

$$q_b = q \mp \frac{2}{5}$$

and the sequence of phase spreads is $q_a\ q_b\ q_a\ q_b\ q_b$. The sequence of phase spreads in the same phase is now different, $q_a\ q_a\ q_b\ q_b\ q_b$. The winding factor and the angle β_ν are

$$\xi_\nu = -\frac{\sin\left(\frac{\nu}{p}\frac{\pi}{2m}\right)}{5q\sin\left(\frac{\nu}{p}\frac{\pi}{10mq}\right)}\sin\left(\frac{\nu}{p}\frac{y}{mq}\frac{\pi}{2}\right) \qquad \text{for odd } \nu/p \qquad (31)$$

$$\xi_\nu = \frac{\sin\left(\frac{\nu}{p}\frac{\pi}{2m} - \frac{\nu}{p}\pi\right)}{5q\sin\left(\frac{\nu}{p}\frac{\pi}{10mq} \pm \frac{\nu}{p}2\pi\right)}\sin\left(\frac{\nu}{p}\frac{y}{mq}\frac{\pi}{2}\right) \qquad \text{for fractional } \nu/p \qquad (32)$$

$$\beta_\nu = \frac{\pi}{2}\frac{1}{m}\frac{\nu}{p}\left(\frac{1}{q} - 1 \pm \frac{4}{5q} - 2m\right) \qquad \text{for any } \nu/p \qquad (33)$$

c) $q = K \pm 2/5$. The numbers of slots per pole per phase are the same as under b), but the sequence of phase spreads is now $q_a\ q_a\ q_b\ q_b\ q_b$. The sequence of phase spreads in one phase is $q_a\ q_b\ q_a\ q_b\ q_b$. The winding factor and the angle β_ν are

$$\xi_\nu = -\frac{\sin\left(\frac{\nu}{p}\frac{\pi}{2m}\right)}{5q\sin\left(\frac{\nu}{p}\frac{\pi}{10mq}\right)}\left[2\cos\left(\frac{\nu}{p}\frac{\pi}{5mq}\right) - 1\right]\sin\left(\frac{\nu}{p}\frac{y}{mq}\frac{\pi}{2}\right) \qquad \text{for odd } \nu/p \qquad (34)$$

$$\xi_\nu = \frac{\sin\left(\frac{\nu}{p}\frac{\pi}{2m} - \frac{\nu}{p}\pi\right)}{5q\sin\left(\frac{\nu}{p}\frac{\pi}{10mq} \pm \frac{\nu}{p}2\pi\right)}\left[2\cos\left(\frac{\nu}{p}\frac{\pi}{5mq} + \frac{\nu}{p}4\pi\right) - 1\right]\sin\left(\frac{\nu}{p}\frac{y}{mq}\frac{\pi}{2}\right) \qquad (35)$$

for fractional ν/p

$$\beta_\nu = \frac{\pi}{2}\frac{1}{m}\frac{\nu}{p}\left(\frac{1}{q} - 1 \mp \frac{6}{5q} - 2m\right) \qquad \text{for any } \nu/p \qquad (36)$$

Fractional-slot winding, arbitrary N

The absolute value of the winding factor can be represented by a universally applicable equation. However, the sign of the winding factor and the phase of the harmonic cannot be ascertained thereby.

For every double-layer winding having $q = K \pm 1/N$ and for all the other windings having phase spreads distributed as uniformly as possible over the machine's periphery, such as e.g. the manner presented for the winding with N = 5 under b) above,

$$|\xi_\nu| = \left| \frac{\sin\left(\frac{\nu}{p}\frac{\pi}{2m}\right)}{Nq\sin\left(\frac{\nu}{p}\frac{\pi}{2Nmq}\right)} \sin\left(\frac{\nu}{p}\frac{y}{mq}\frac{\pi}{2}\right) \right| \qquad \text{for odd } \nu/p \qquad (37)$$

The winding factor obtains, also for fractional and even-numbered harmonics, only the same values as for odd harmonics. The same values recur at a uniform spacing with respect to $|\nu/p|$.

3.2.1.2 Single-layer windings

Single-layer windings may also have the same values of N as double-layer windings. For reasons of manufacturing technique, however, usually only integer-slot windings or fractional-slot windings with N = 2 are made. Accordingly, the following considerations are confined to such windings. In addition, of the fractional-slot windings only the three-phase variety is considered, since they are rarely made with a greater number of phases. Two-phase windings are also omitted because they cannot be made symmetrical with a single-layer fractional-slot winding. Fractional-slot windings can be divided into windings with "half coils" and windings with "whole coils".

Equations (16) and (17) are also valid for the m.m.f. of a single-layer winding [23, p. 103]. In contrast, the orders of the m.m.f. harmonics are not always the same as in the corresponding double-layer winding: they depend not only on the value of N but also on the manner in which the winding has been made.

Integer-slot winding

A single-layer integer-slot winding produces the same m.m.f. harmonics as a double-layer integer-slot winding. The equations (19) and (20) of the double-layer winding are also valid for the winding factor and for the angle β_ν of the corresponding single-layer winding.

Fractional-slot winding, N = 2

a) Windings with half coils

Fig. 6 shows an example of a winding with 2,5 slots per pole per phase, two whole coils and one half coil belonging to each coil group. Both half coils of two adjacent coil groups occupy the same slot. The current pattern of the double-layer winding producing the same m.m.f. distribution as the single-layer winding of Fig. 6 is shown for comparison in Fig. 7. Thus, a single-layer winding can be replaced, as regards the m.m.f. harmonics and winding factors, by a double-layer winding, having the coil pitch

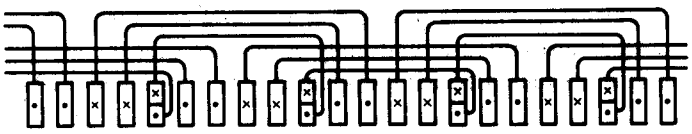

Fig. 6. A single-layer fractional-slot winding with 2,5 slots per pole per phase, made with half coils.

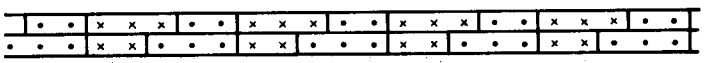

Fig. 7. The current pattern of the double-layer winding corresponding to Fig. 6.

$$y = 3q - \frac{1}{2} \tag{38}$$

The orders of the harmonics are

$$\frac{\nu}{p} = 3g + 1 \qquad g = 0, \pm 1, \pm 2, \ldots \tag{39}$$

The winding factors can be calculated from (21) and (22), taking into account Eq. (38):

$$\xi_\nu = \frac{\sin\left(\frac{\nu}{p}\frac{\pi}{6}\right)}{2q\sin\left(\frac{\nu}{p}\frac{\pi}{12q}\right)} \sin\left(\frac{\nu}{p}\frac{6q-1}{6q}\frac{\pi}{2}\right) \qquad \text{for odd } \nu/p \tag{40}$$

$$\xi_\nu = \pm \frac{\cos\left(\frac{\nu}{p}\frac{\pi}{6}\right)}{2q\cos\left(\frac{\nu}{p}\frac{\pi}{12q}\right)} \sin\left(\frac{\nu}{p}\frac{6q-1}{6q}\frac{\pi}{2}\right) \qquad \text{for even } \nu/p \tag{41}$$

The reference axis must be placed in the centre of the first coil of a given coil group of the corresponding double-layer winding. For the double signs the rule stated after Eq. (23) is valid. Eq. (23) is valid for the angle β_ν.

b) Windings with whole coils

Contrary to the preceding chapter, the winding may also be made, using only whole coils. In that case the winding consists of two types of coil groups, having slot numbers per pole per phase differing by 1. Both coil groups spread over four poles. It follows that the smallest number of poles is four. As an example, a fractional-slot winding with 2,5 slots per pole per phase is shown in Fig. 8. In any one phase, a larger and smaller coil group alternate. The coils of the larger coil group can be considered as composed of coils of constant width, the width of the coils being

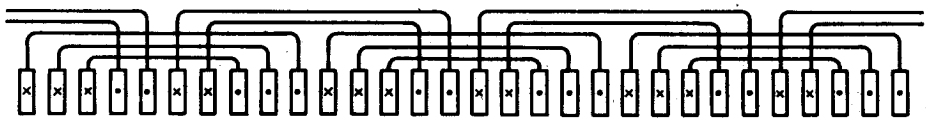

Fig. 8. A single-layer fractional-slot winding with 2,5 slots per pole per phase, made with whole coils.

$$y_1 = 3q - \frac{1}{2} \tag{42}$$

Correspondingly, the coil pitch of the narrower coil group is

$$y_2 = 3q + \frac{1}{2} \tag{43}$$

The orders of harmonics are

$$\frac{\nu}{p} = -\frac{1}{2}(3g + 1) \qquad g = 0, \pm 1, \pm 2, \ldots \tag{44}$$

The winding factor and the angle β_ν are

$$\xi_\nu = \frac{\sin\left(\frac{\nu}{p}\frac{\pi}{6}\right)}{2q\sin\left(\frac{\nu}{p}\frac{\pi}{12q}\right)} \sin\left(\frac{\nu}{p}\frac{6q-1}{6q}\frac{\pi}{2}\right) \qquad \text{for odd } \nu/p \tag{45}$$

$$\xi_\nu = \frac{\cos\left(\frac{\nu}{p}\frac{\pi}{6}\right)}{2q\cos\left(\frac{\nu}{p}\frac{\pi}{12q}\right)} \sin\left(\frac{\nu}{p}\frac{6q-1}{6q}\frac{\pi}{2}\right) \qquad \text{for even } \nu/p \tag{46}$$

$$\xi_\nu = \mp \frac{\sin\left(\frac{\nu}{p}\frac{\pi}{3}\right)}{2q} = \mp \frac{1}{4q} \qquad \text{for fractional } \nu/p \tag{47}$$

$$\beta_\nu = \frac{\pi}{6}\frac{\nu}{p}\left(\frac{1}{q} - 1 \mp \frac{1}{2q}\right) \qquad \text{for any } \nu/p \tag{48}$$

Of the double signs, the upper sign is chosen when the reference axis lies in the centre of the larger phase spread, and the lower sign when the reference axis is placed in the centre of the smaller phase spread.

3.2.2 Slot harmonics

The winding factor is a periodic function with regard to the order of the harmonic. The values of the winding factor are regularly recurring. Harmonics having a winding factor equal to that of the fundamental are called slot harmonics. Their orders are [23, p. 96]

$$\frac{\nu}{p} = 2mqg + 1 = \frac{Q}{p} g + 1 \qquad g = \pm 1, \pm 2, \ldots \tag{49}$$

where Q is the number of slots.

Slot harmonics always occur in pairs. The pair of waves obtained from Eq. (49) with $g = \pm 1$ is called the first slot harmonic. Correspondingly, the second slot harmonic is obtained with $g = \pm 2$. One wave of the pair rotates in the same direction as the fundamental, and the other rotates in the opposite direction.

3.3 HARMONICS OF FLUX DENSITY DISTRIBUTION DUE TO THE PERMEANCE VARIATIONS

3.3.1 Harmonics due to rotor eccentricity

Consider the flux density harmonics which appear in an air-gap when the permeance variations are exclusively due to the rotor eccentricity.

Two border-line cases of the rotor eccentricity may be distinguished, which invariably occur simultaneously in practice, but of which one may be the decisive factor. The rotor may be concentric with regard to the shaft but eccentric in the air-gap, as shown in Fig. 9 a (so-called static eccentricity). The other border-line case is that of eccentricity of the rotor with regard to the shaft, combined with concentric placement of the shaft in the air-gap, Fig. 9 b (so-called dynamic eccentricity).

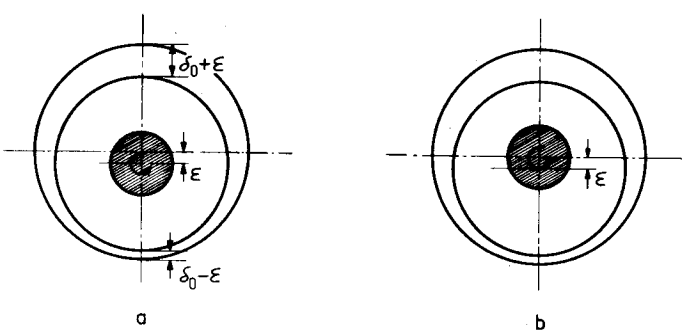

Fig. 9. a) A statically eccentric rotor. b) A dynamically eccentric rotor.

In the case of Fig. 9 a the length of the air-gap, in rotor reference frame, is a function of space and time. In the case of Fig. 9 b, again, the lenght of the air-gap in the rotor reference frame is not time-dependent, but only a function of space. We denote the distance between the centres of the rotor and of the stator bore by ϵ. Then the air-gap conforms to a curve of the kind shown in Fig. 10. If ϵ is small, compared with the air-gap diameter, the specific permeance of the air-gap in the rotor reference frame is roughly

$$\Lambda = \frac{\mu_0}{\delta_0 - \epsilon\cos(\vartheta_2 + \omega_\epsilon t - \varphi_\epsilon)} \tag{50}$$

where δ_0 is the mean air-gap length and φ_ϵ the (mechanical) angle shown in Fig. 10. When the eccentricity is static, the angular frequency ω_ϵ equals the rotor speed which is ω/p in synchronous operation. In the case of dynamic eccentricity, ω_ϵ is zero.

In order to express (50) as a series, as in (5), Λ is expanded into a Taylor series:

$$\Lambda = \frac{\mu_0}{\delta_0}\left\{1 + \frac{\epsilon}{\delta_0}\cos(\vartheta_2 + \omega_\epsilon t - \varphi_\epsilon) + \left(\frac{\epsilon}{\delta_0}\right)^2 \frac{1}{2}\left[1 + \right.\right.$$
$$\left.\left. + \cos(2\vartheta_2 + 2\omega_\epsilon t - 2\varphi_\epsilon)\right] + \cdots\right\}$$

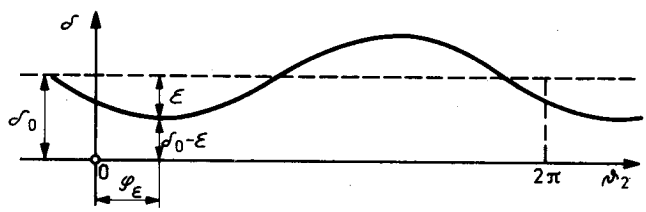

Fig. 10. The air-gap length of an eccentric rotor.

The series converges if $\epsilon < \delta_0$. If ϵ/δ_0 is small, the higher powers of ϵ/δ_0 may be ignored and Λ is roughly

$$\Lambda = \frac{\mu_0}{\delta_0}\left[1 + \frac{\epsilon}{\delta_0}\cos(\vartheta_2 + \omega_\epsilon t - \varphi_\epsilon)\right] \tag{51}$$

The sum of the linear current density distributions produced by the stator and rotor windings may be represented by a series in accordance with (2), Considering only those harmonics which a stator winding can produce, the angular frequency in the rotor reference frame is

$$\omega_\nu = \left(1 - \frac{\nu}{p}\right)\omega$$

and the νth linear current density harmonic is

$$a_\nu = -\hat{a}_\nu \sin\left[\nu\vartheta_2 - \left(1 - \frac{\nu}{p}\right)\omega t - \varphi_\nu\right] \tag{52}$$

Those current harmonics which fulfill the condition $\nu \pm 1 \neq 0$ produce, together with the specific permeance (51), flux density harmonics in accordance with (7) and (8):

$$b_{\mathrm{I}} = \sum_\nu \hat{b}_\nu \cos\left[\nu\vartheta_2 - \left(1 - \frac{\nu}{p}\right)\omega t - \varphi_\nu\right] \tag{53}$$

$$b_{\mathrm{II}} = \sum_\nu \frac{\epsilon}{2\delta_0}\hat{b}_\nu \cos\left\{(\nu \pm 1)\vartheta_2 - \left[\left(1 - \frac{\nu}{p}\right)\omega \pm \omega_\epsilon\right]t - (\varphi_\nu \pm \varphi_\epsilon)\right\} \tag{54}$$

The amplitude of the νth harmonic is

$$\hat{b}_\nu = r\Lambda_0 \frac{\hat{a}_\nu}{\nu} = \frac{\mu_0}{\delta_0}\frac{r\hat{a}_\nu}{\nu} = \frac{\mu_0}{\delta_0}\hat{v}_\nu \tag{55}$$

where $\hat{v}_\nu$ is obtained from (17). When calculating the fundamental ($\nu = p$) the sum of the stator current and the rotor current referred to the stator is substituted in (17) for the current I; otherwise ($\nu > p$) the stator current only is inserted. It is then assumed that the rotor does not suppress the harmonics produced by the stator winding.

The harmonics of Eq. (53) are harmonics appearing in the constant δ_0 air-gap. Eq. (54) represents the additional harmonics caused by eccentricity.

Integer-slot windings always fulfill the condition $\nu \pm 1 \neq 0$ if the number of pole pairs is greater than 1. In contrast, fractional-slot windings may also produce sub-harmonics having a pole pair number = 1, while the pole pair number of the machine is > 1. In this case, and always if the pole pair number of the machine is 1, there exist harmonics in accordance with (9) and (10):

$$b_{III} = \frac{\epsilon}{2\delta_0} \hat{b}_1 \cos\left\{2\vartheta_2 - \left[\left(1 - \frac{1}{p}\right)\omega + \omega_\epsilon\right]t - (\varphi_1 + \varphi_\epsilon)\right\} \tag{56}$$

$$b_{IV} = -\frac{1}{4}\left(\frac{\epsilon}{\delta_0}\right)^2 \hat{b}_1 \cos\left\{\vartheta_2 - \left[\omega_\epsilon \pm \left[\left(1 - \frac{1}{p}\right)\omega - \omega_\epsilon\right]\right]t + [\varphi_\epsilon \pm (\varphi_1 - \varphi_\epsilon)]\right\} \tag{57}$$

$\hat{b}_1$ is the amplitude of that harmonic present in the constant δ_0 air-gap whose pole pair number is 1, and it can be calculated from (55). Accordingly, in two-pole machines $\hat{b}_1$ is the amplitude of the fundamental.

The fundamental flux density wave is stationary with reference to the rotor. In contrast, the harmonics produced by the eccentricity (Eq. 54 $\nu = p$)

$$b_{II} = \frac{\epsilon}{2\delta_0} \hat{b}_p \cos\left[(p \pm 1)\vartheta_2 \mp \omega_\epsilon t - (\varphi_p \pm \varphi_\epsilon)\right] \tag{58}$$

have an angular frequency ω_ϵ in the rotor reference frame. When dynamic eccentricity is concerned, ω_ϵ is zero, while in the case of static eccentricity ω_ϵ equals ω/p. The frequency diminishes rapidly with increasing pole number. The amplitude of the harmonic can be made rather high on the other hand. It should thus be possible, in high-speed machines, to use the harmonic (58) to produce the excitation voltage component proportional to the fundamental of the flux density distribution.

According to the foregoing, the stator winding produces harmonics proportional to the load current which are now, with eccentric rotor, represented by Eq. (53). The permeance harmonics caused by the eccentricity, too, produce flux density harmonics which are proportional to the load current (Eq. (54), $\nu > p$). However, the amplitudes $\epsilon/(2\delta_0 \hat{b}_\nu)$ of these harmonics are smaller than those ($\hat{b}_\nu$) of the harmonics due to the stator winding distribution. The angular frequencies of the harmonics produced by the permeance variations and of those produced by the stator winding differ little if the pole numbers are closely equal. It is therefore manifestly unprofitable to use the harmonics proportional to the load current, produced by the eccentricity, for generating an excitation voltage.

In the cases in which the stator winding develops a m.m.f. harmonic with pole pair number 1, harmonics in accordance with (56) and (57) are also produced. Owing to the great wave-length, the field winding suppresses these harmonics so that they are not proportional to the load current. They are proportional to the fundamental of the flux distribution in two-pole machines, in which case and with static eccentricity, they might

be used to produce the excitation voltage component which should be proportional to the fundamental of the flux density wave. In the case of dynamic eccentricity the angular frequency of these harmonics is zero with reference to the rotor.

3.3.2 Harmonics due to saturation

Consider the flux density harmonics which appear in an air-gap when the variations of permeance are due to saturation alone.

Owing to saturation, the permeability of iron varies from tooth to tooth. The saturation can be taken into account by increasing the actual air-gap (δ) so much that, imagining the m.m.f. of the entire magnetic circuit as acting on this increased, so-called equivalent air-gap (δ''), the flux density distribution in the equivalent air-gap equals that in the actual air-gap.

The saturation of the stator and rotor yokes can be taken into account by adding to the air-gap length a constant δ_s, Fig. 11. The teeth reach their highest saturation close to the peak value of the flux density. Accordingly, the air-gap has its largest apparent length at this point, Fig. 12. The permeance harmonics due to saturation have the same speed as the fundamental of the flux density wave. It follows that the specific permeance of the air-gap may be formally written in the rotor reference frame as

$$\Lambda = \Lambda_0 + \sum_{\mu} \hat{\Lambda}_\mu \cos(\mu\vartheta_2 - \varphi_\mu) \tag{59}$$

where $\mu = k \cdot 2p$, $k = 1, 2, 3, \ldots$

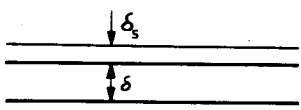

Fig. 11. The apparent increase of the air-gap due to saturation of the yoke.

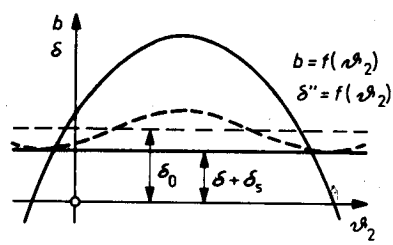

Fig. 12. The apparent increase of the air-gap due to saturation of the teeth.

The resulting linear current density wave (52) due to the stator and rotor windings produces, with the specific permeance (59), harmonics in accordance with (7) and (8):

$$b_{\mathrm{I}} = \sum_{\mu} \hat{b}_\nu \cos\left[\nu\vartheta_2 - \left(1 - \frac{\nu}{p}\right)\omega t - \varphi_\nu\right]$$

$$b_{\mathrm{II}} = \sum_{\substack{\nu \\ \nu \neq \pm\mu}} \sum_{\mu} \frac{1}{2} \hat{b}_\nu \frac{\hat{\Lambda}_\mu}{\Lambda_0} \cos\left[(\nu \pm \mu)\vartheta_2 - \left(1 - \frac{\nu}{p}\right)\omega t - (\varphi_\nu \pm \varphi_\mu)\right]$$

Eq. (55) is valid for $\hat{b}_\nu$. Fractional-slot windings may produce even-numbered harmonics, in which case $\nu \pm \mu$ may also be zero (μ is an even number). Then there exist in the air-gap, in addition to the preceding flux density waves, harmonics (9) and (10):

$$b_{III} = -\sum_{\substack{\mu \\ (\nu=\pm\mu)}} \pm \frac{1}{2}\hat{b}_{\pm\mu}\frac{\hat{\Lambda}_\mu}{\Lambda_o}\cos\left[\pm 2\mu\vartheta_2 - \left(1 - \frac{\pm\mu}{p}\right)\omega t - (\varphi_{\nu=\pm\mu} \pm \varphi_\mu)\right]$$

$$b_{IV} = -\sum_{\lambda}\sum_{\substack{\mu \\ (\nu=\pm\mu)}} \pm \frac{1}{4}\hat{b}_{\pm\mu}\frac{\hat{\Lambda}_\mu\hat{\Lambda}_\lambda}{\Lambda_o}\cos\left\{\lambda\vartheta_2 \mp \left(1 - \frac{\pm\mu}{p}\right)\omega t - [\varphi_\lambda \pm (\varphi_{\nu=\pm\mu} \mp \varphi_\mu)]\right\}$$

Of the double signs, the upper ones are valid for the permeance harmonics having a pole pair number $\mu = \nu$, and the lower signs are valid for those harmonics with a pole pair number $\mu = -\nu$.

The angular frequency of the fundamental of the flux density wave and that of the harmonics proportional to the fundamental ($\nu = p$) in the rotor reference frame is zero for all wave groups ($b_I \cdots b_{IV}$). Therefore it is not possible, with the aid of saturation, to obtain an excitation voltage component proportional to the fundamental.

The harmonics of the air-gap m.m.f. produce together with the permeance harmonics, flux density harmonics proportional to the stator current, which are represented by the wave groups $b_{II} \cdots b_{IV}$ ($\nu > p$). However, the amplitudes of these harmonics are small.

3.3.3 Harmonics due to salient-pole rotor

When the stator is smooth and the rotor has salient poles a similar expression as that for saturation (Eq. (59)) is also valid for the specific air-gap permeance. The pole pairs of the permeance harmonics are also the same as in conjunction with saturation harmonics, i.e., $\mu = k \cdot 2p$ ($k = 1, 2, 3, \ldots$). The flux density harmonics are then of the same type as the harmonics produced by saturation. For the same reasons as in the case of saturation harmonics, the flux density harmonics due to saliency are not suitable for producing an excitation voltage either.

3.3.4 Harmonics due to slot openings

3.3.4.1 Slotted stator

Consider first the flux density harmonics due to the slot openings of the stator. The rotor is assumed to be smooth and the permeability of iron infinite.

The maximum value of the permeance occurs at the centre of the tooth and the minimum value at the centre of the slot opening. It follows that the pole pair numbers of permeance harmonics are multiples of the slot number. The angular frequency is zero in the stator reference frame, and hence the specific permeance may be formally written as

$$\Lambda = \Lambda_o + \sum_k \hat{\Lambda}_{kQ1}\cos(kQ_1\vartheta_1 - \varphi_{kQ1}) \qquad k = 1, 2, 3, \ldots \qquad (60)$$

In the rotor reference frame the specific permeance is, according to the transformation (15),

$$\Lambda = \Lambda_o + \sum_k \hat{\Lambda}_{kQ1} \cos\left(kQ_1\vartheta_2 + \frac{kQ_1}{p}\,\omega t - \varphi_{kQ1}\right) \tag{61}$$

The mean value of the specific permeance is

$$\Lambda_o = \frac{\mu_o}{k_{c1}\delta}$$

where k_{c1} is Carter's coefficient of the stator and δ the air-gap length at the tooth.

The resulting linear current density wave (52) due to the stator and rotor windings produce harmonics together with the specific permeance (61) in accordance with (7) and (8):

$$b_I = \sum_\nu \hat{b}_\nu \cos\left[\nu\vartheta_2 - \left(1 - \frac{\nu}{p}\right)\omega t - \varphi_\nu\right]$$

$$b_{II} = \sum_\nu \sum_k \frac{1}{2}\,\hat{b}_\nu \frac{\hat{\Lambda}_{kQ1}}{\Lambda_o} \cos\left[(\nu \pm kQ_1)\vartheta_2 - \left(1 - \frac{\nu}{p} \mp \frac{kQ_1}{p}\right)\omega t - (\varphi_\nu \pm \varphi_{kQ1})\right] \tag{62}$$

These equations contain all harmonics produced, because the symmetrical integer- and fractional-slot windings under consideration cannot produce any harmonics in accordance with (9) and (10) which occur when $\nu \pm kQ_1 = 0$. This can be seen as follows.

A symmetric double-layer winding produces m.m.f. harmonics in accordance with (12) and (13):

$$\frac{\nu}{p} = \frac{1}{N}(2mg + c)$$

where c = 2 for even N and c = 1 for odd N. For simplicity the double signs in Eqs. (12) and (13) are omitted, since they have no effect on the result. Expressing Q_1 in the form

$$Q_1 = 2pm\,\frac{T}{N}$$

we obtain

$$\nu \pm kQ_1 = \frac{p}{N}(2mg + c) \pm k \cdot 2pm\,\frac{T}{N}$$

Equating $\nu \pm kQ_1$ to zero and resolving for g we get

$$g = \pm kT - \frac{c}{2m}$$

Since k and T are integers and c is either 1 or 2, and $m > 1$, g is always a fractional number. Therefore there exists no such integer g and also no such m.m.f. harmonic for which $\nu \pm kQ_1 = 0$. In the same way it can be demonstrated that also a single-layer winding cannot produce a m.m.f. harmonic with $\nu \pm kQ_1 = 0$.

The slot openings produce m.m.f. harmonics in accordance with (62). For $\nu = p$ the numbers of harmonic pole pairs $p \pm kQ_1$ are same as those of the pole pairs of slot

harmonics due to the winding distribution, Eq. (49). The harmonics due to slot openings rotate at the same speed as the slot harmonics and both types therefore affect each other. All the other harmonics due to slot openings ($\nu \neq p$), too, are superposed on the harmonics due to the stator winding distribution. This can be seen as follows.

According to the foregoing a double-layer winding produces harmonics

$$\frac{\nu}{p} = \frac{1}{\mathrm{N}} (2mg + \mathrm{c})$$

One of these, say ν', generates together with the kQ_1th permeance harmonic flux density harmonics

$$\nu' \pm kQ_1 = \frac{p}{\mathrm{N}} (2mg' + \mathrm{c}) \pm k \cdot 2pm \frac{\mathrm{T}}{\mathrm{N}}$$

Another harmonic due to the winding distribution, say ν, has the same number of pole pairs as $\nu' \pm kQ_1$ i.e., $\nu = \nu' \pm kQ_1$. Therefore,

$$\frac{p}{\mathrm{N}} (2mg + \mathrm{c}) = \frac{p}{\mathrm{N}} (2mg' + \mathrm{c}) \pm k \cdot 2pm \frac{\mathrm{T}}{\mathrm{N}}$$

and resolving for g

$$g = g' \pm kT$$

For every integer g there exists an infinite number of integer pairs g', k which satisfy this equation. Then also for every harmonic ν produced by the stator winding distribution there exists an infinite number of harmonics produced by slot openings whose pole pair number $\nu' \pm kQ_1$ equals ν. The harmonics produced by slot openings have the angular frequency in the rotor reference frame, according to (62),

$$\omega' = \left(1 - \frac{\nu'}{p} \pm \frac{kQ_1}{p}\right) \omega = \left(1 - \frac{\nu}{p}\right) \omega$$

that is, the angular frequency equals that of the νth harmonic. An infinite number of harmonics due to slot openings is therefore superposed on the harmonics produced by the stator winding distribution. It is also seen from the foregoing that the slot openings produce only those harmonics which are due to the stator winding distribution. In the same way it can be shown that when the stator winding is a single-layer winding the slot openings produce only those harmonics which the stator winding generates.

ZWEYGBERGK [26, p. 55] has demonstrated that the resulting slot harmonic is composed of the slot harmonic due to the stator winding distribution, on which an infinite number of harmonics due to the slot openings is superposed. This phenomenon is accordingly also encountered with harmonics other than the slot harmonics.

For calculating a fixed slot harmonic, an infinite number of harmonics has to be geometrically added. Owing of the different amplitudes and phases of these harmonics it is difficult to write a closed expression for the slot harmonics. In each individual case, however, the amplitude of the resulting slot harmonic can be calculated from (62), taking into account a large enough number of terms. Taking into account only the first term may result in a considerable error, as ZWEYGBERGK [26, p. 57] has shown.

Concerning the calculation of amplitudes of the permeance harmonics due to the slot openings numerous papers have been written, which may be divided into three groups. In the first group the solution is accomplished graphically with the aid of an orthogonal field map or by experimental measurements. In the second group the specific permeance is assumed to conform to a simple function, e.g. a square wave, wherein the specific permeance is zero at the slot opening [9], or has there a small constant value [12] and has the value μ_0/δ at the tooth. In the third group the solution is based on the conformal mapping. In these cases it is always assumed that the air-gap diameter, the depth of the slot and the permeability of iron are infinite. In practice the depth of the slot can be regarded infinite if it exceeds 1,5 times the slot opening [6]. By conformal mapping, however, no explicit permeance function can be obtained. On the other hand, closed expressions can be derived for the minimum and mean values of the permeance. Between the minimum and the maximum (μ_0/δ) located at the centre of the slot and at the centre of the tooth, respectively, WEBER [25] has assumed the specific permeance to conform to the function $\sin^{2n}(Q_1\vartheta_1)$, where

$$n = \frac{t_1}{x_{41}} - 1$$

rounded to the nearest integer, t_1 the tooth pitch and x_{41} the width of the slot opening. This function can be expanded into a finite series resembling a Fourier series when n is an integer. The ratio of the amplitude to the mean value of the specific permeance is [8, p. 142]

$$\frac{\hat{\Lambda}_{kQ1}}{\Lambda_o} = -(-1)^k \cdot 2(k_c - 1)\frac{\binom{2n}{n-k}}{\binom{2n}{n}} \tag{63}$$

Carter's coefficient is calculated from

$$k_c = \frac{1}{1 - \tau\beta} \tag{64}$$

in this case, where τ is a function of t_1/x_{41} and β a function of x_{41}/δ, Fig. 13.

Although the permeance function cannot be gained in an explicit form by conformal mapping, this may be numerically accomplished. The families of curves in Figs. 14···17 have been calculated by FREEMAN [6]. In these the interaction of adjacent slots has been taken into account. The families of curves have been presented in terms of relative values. The ordinate $\hat{\Lambda}_{kQ1}/\Lambda_0$ is the amplitude of the harmonic, divided by the mean value. In the curves representing the mean value of permeance (Fig. 14), the ordinate is $\Lambda_0/(\mu_0/\delta)$, i.e., the inverse of Carter's coefficient. The abscissa x_{41}/t_1 is the ratio of slot opening to tooth pitch, and the parameter x_{41}/δ is the slot opening to air-gap ratio. With semi-closed slots, saturation of iron ensues first in the tips of the tooth. This can be taken into account by enlarging the slot opening. This so-called equivalent slot opening is approximately calculable by the method described by NORMAN [16]. The largest slot opening appears between the teeth in which the flux has its maximum. It follows that the magnitude of the equivalent slot opening varies from tooth to tooth. ZWEYGBERGK [26, p. 62] has shown that, although the saturation of the tooth tips has an effect on the air-gap permeance, it does not influence the slot harmonics. This is supported by

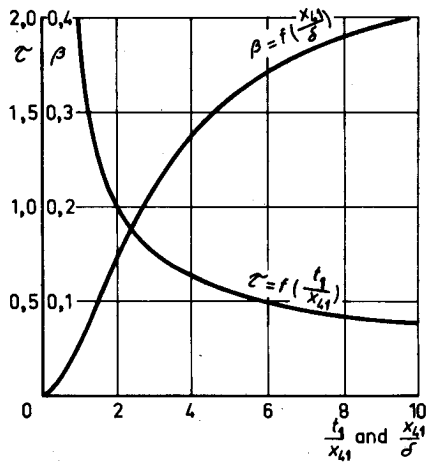

Fig. 13. Functions τ and β in Eq. (64).

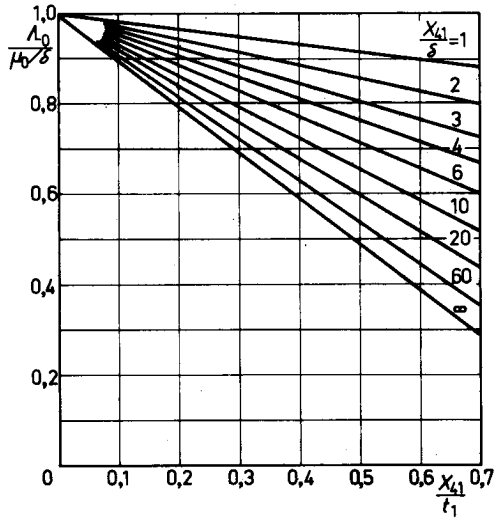

Fig. 14. The mean value of the specific air-gap permeance.

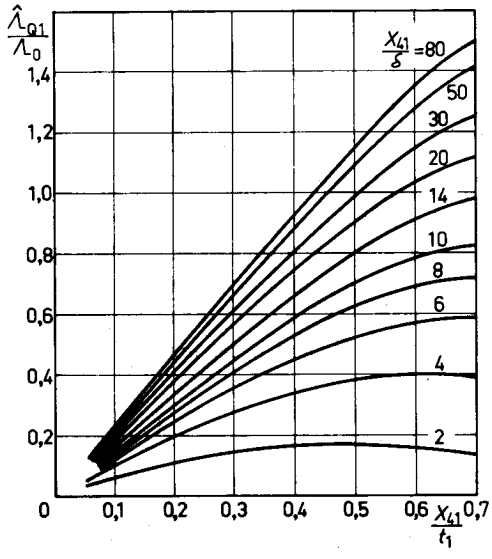

Fig. 15. The first harmonic of the specific air-gap permeance due to slotting.

measurements performed by KEHSE [10] and FROHNE [8]. In contrast, saturation of the teeth has a considerable effect on Carter's coefficient and thereby on the amplitudes of the fundamental and of the lower harmonics.

FROHNE measured [8] the first three harmonics due to slotting in a test machine. He verified that Weber's method gives results in fair agreement with measurements (error about 10 %). A simple square-wave permeance function, in which the specific permeance is assumed to be zero at the slot opening and constant at the tooth, also yields satisfactory results for the first slot harmonic (error −10···−20 %). For higher harmonics the

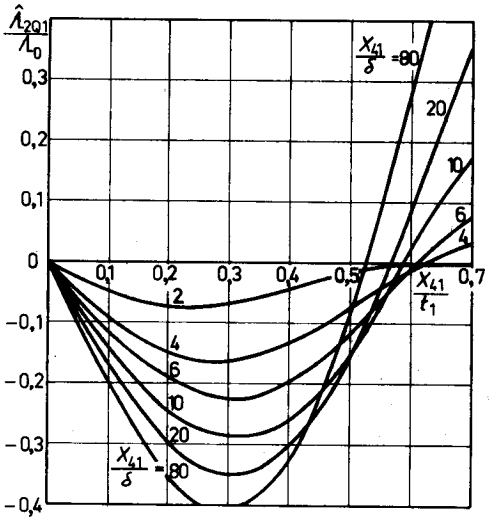

Fig. 16. The second harmonic of the specific air-gap permeance due to slotting.

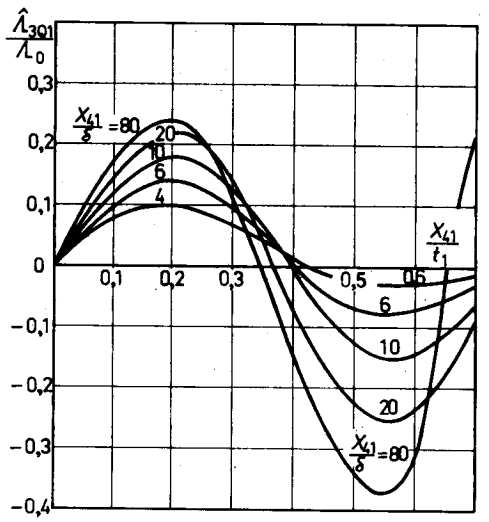

Fig. 17. The third harmonic of the specific air-gap permeance due to slotting.

method is useless, however. FREJTICH and SIEGL [7] verified by measurements that the curves calculated by FREEMAN [6] produce values in close agreement with measurements.

Excitation voltage component proportional to the fundamental of the flux density distribution is obtainable from the harmonics (62) produced by the stator slot openings ($\nu = p$). A disadvantage of these harmonics is the large number of pole pairs ($p \pm kQ_1$) in that the small pole pitch may cause difficulties in manufacture. Secondly, these harmonics have a high angular frequency $kQ_1\,\omega/p$ and the reactance of the auxiliary winding may therefore attain a high value. An advantage of these harmonics is their high amplitude, which is easily altered at the design stage by changing the width of the slot opening.

From the harmonics (62) produced by the slotting it is also possible to obtain an excitation voltage component proportional to the stator current ($\nu \neq p$). The amplitudes of the harmonics are small, however.

3.3.4.2 Slotted rotor

When the stator is smooth and slot openings are only provided in the rotor, Eq. (60) is valid for the specific air-gap permeance if ϑ_2 and Q_2 are substituted for ϑ_1 and Q_1. The equation thus obtained has the same form as the specific permeance function (59) due to the saturation. Hence, for the same reasons as in the case of saturation, it is not possible to obtain an excitation voltage component proportional to the fundamental of the flux density distribution, and the amplitudes of the harmonics proportional to the stator current are small.

3.3.4.3 Slotted stator and rotor

ZWEYGBERGK [26, p. 60] has presented an approximate method for determining the specific air-gap permeance when there are slots in the stator and rotor both. According to him, the specific air-gap permeance contains harmonics $|k_1Q_1 \pm k_2Q_2|$ in addition to the pole pairs k_1Q_1 and k_2Q_2 appearing when the stator or rotor alone is slotted. The νth m.m.f. harmonic produces together with the specific permeance the same harmonics as in one-sided slotting and, in addition, harmonics with pole pairs $\nu \pm |k_1Q_1 \pm k_2Q_2|$ and having the angular frequency $|1 - (\nu \pm k_1Q_1)/p|\omega$ in the rotor reference frame. The upper sign in the expression of the angular frequency and the first double sign in that of the pole pair number are simultaneously valid, as are also the lower signs. The second double sign in the pole pair number can be arbitrarily chosen, whereby four harmonics in all are obtained. The permeance harmonics $|k_1Q_1 \pm k_2Q_2|$ due to double-sided slotting are small as regards their amplitude, because they are proportional to the product of two amplitudes of permeance harmonics, which are usually small in practice [26, p. 60].

3.3.5 Harmonics due to shaped stator air-gap face

Permeance harmonics of the same kind as those due to stator slot openings are also produced when the stator is salient or deviates in other ways from a smooth surface, as illustrated by Fig. 18. In Fig. 18 a the stator surface is undulating. In Fig. 18 b, open slots regularly alternate with very small slot openings or totally closed slots. A third possibility would be to provide the stator with slot wedges, some of them magnetic conductors and other ones non-magnetic.

The solution according to Fig. 18 a involves high manufacturing costs. However, any required permeance wave having a desired lenght and height is thereby easily obtained. Furthermore, the harmonic content of the permeance can be kept low by means of an appropriate design.

The solution seen in Fig. 18 b is simple as regards the manufacturing process. A study is made in the following concerning the kind of harmonics, referring to their order and angular frequency, which can possibly be produced by this method.

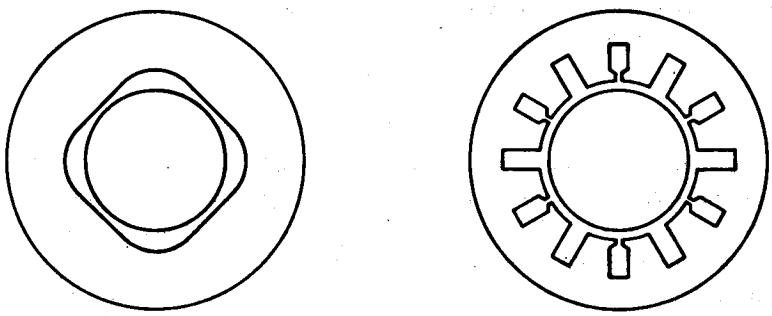

a b

Fig. 18. Two means to produce permeance variations by shaping the stator air-gap face: a) an undulating air-gap surface, b) partly open and partly semi-closed slots.

Let Q_a be the number of open slots. These slots are spaced at a regular distance. The intervening slots are closed. The open slots produce permeance harmonics with kQ_a pole pairs, which in their turn, together with the fundamental m.m.f. wave give rise to harmonics $p \pm kQ_a$. One of these is desired to have the same wave-length as the νth harmonic due to the stator winding distribution, that is

$$p \pm kQ_a = \nu$$

Resolving for Q_a,

$$Q_a = \left| \frac{p}{k} \left(\frac{\nu}{p} - 1 \right) \right| \tag{65}$$

The ratio of all stator slots Q_1 to Q_a

$$\frac{Q_1}{Q_a} = \frac{2mqk}{\left| \frac{\nu}{p} - 1 \right|} \tag{66}$$

has to be an integer to make the open slots recur at regular intervals. When a three-phase stator winding is concerned and the fundamental of the permeance wave ($k = 1$) is considered, the following ratio has to be an integer:

$$\frac{Q_1}{Q_a} = \frac{6q}{\left| \frac{\nu}{p} - 1 \right|} \tag{67}$$

For an integer-slot winding

$$\frac{\nu}{p} = 6g + 1 \qquad (g = 0, \pm 1, \pm 2, \ldots)$$

hence

$$\frac{Q_1}{Q_a} = \frac{q}{|g|}$$

When the stator carries a three-phase integer-slot winding, the number of slots per pole per phase must be divisible by g to give an integer Q_1/Q_a. For instance for $g = \pm 1$, producing the -5th and $+7$th harmonics, every qth slot has to be open. All harmonics cannot be produced by this method if we confine ourselves to the fundamental of the permeance wave. For instance, with $q = 3$ the -11th and $+13$th harmonics, for which $g = \pm 2$, are not obtainable.

For a three-phase fractional-slot winding with $N = 2$,

$$\frac{\nu}{p} = 3g + 1 \qquad (g = 0, \pm 1, \pm 2, \ldots)$$

hence

$$\frac{Q_1}{Q_a} = \frac{2q}{|g|} = \frac{T}{|g|}$$

It follows that the numerator T of the slots per pole per phase figure has to be divisible by g. The − 2nd and + 4th harmonics are obtained with g = ± 1. In this case every Tth slot must be open. The − 5th and + 7th harmonics are produced when g = ± 2. Being an odd number T is not divisible by 2, and the fundamental of the permeance wave is not able to produce the − 5th and + 7th harmonics.

The angular frequency of the harmonics $p \pm kQ_a$ produced by the permeance harmonics together with the fundamental m.m.f. wave is, in the rotor reference frame

$$\omega_{p \pm kQa} = \frac{kQ_a}{p}\,\omega = \left|\frac{\nu}{p} - 1\right|\omega \tag{68}$$

The angular frequency therefore equals that of the νth harmonic due to the stator winding.

It is thus found that by using closed and open slots in the stator the permeance harmonics due to the slotting may be utilized in producing harmonics having pole pairs and angular frequencies equal to those of the harmonics due to the stator winding distribution.

3.4 APPLICABILITY OF HARMONICS IN PRODUCING EXCITATION VOLTAGE

It has been shown above that the permeance variations due to the slot openings of the stator, or more generally to irregularities of the stator's air-gap face produce flux density harmonics proportional to the fundamental of the flux density distribution and travelling with reference to the rotor. Furthermore, the static eccentricity of the rotor produces harmonics proportional to the fundamental of the flux density distribution. The other harmonics proportional to the fundamental all rotate at the rotor speed. Since the static eccentricity, as viewed from the rotor, may also be considered an irregularity of the stator face, the excitation voltage component proportional to the fundamental is only obtainable by the aid of permeance variations due to irregularities of the stator face.

The m.m.f. harmonics produce, together with the constant component of the permeance wave, flux density harmonics (harmonics due to the stator winding distribution), which are proportional to the stator current. By the aid of these harmonics the second requisite component of excitation voltage may thus be obtained. The m.m.f. harmonics also produce, together with the harmonic content of the permeance, flux density harmonics proportional to the stator current, but the amplitudes of these harmonics are small.

In order to obtain self-regulation it is required, in addition to the proportionalities presented above, that the phase difference between the two components of the excitation voltage is $90^\circ + \varphi$. It is investigated in the following whether it is possible to obtain this required phase difference with the aid of the harmonics due to the slotting and of the slot harmonics due to the stator winding distribution.

When the stator reference frame is placed to have its origin at the centre of a stator slot, it can be shown [2] that the angle β_ν in the m.m.f. equation (14) is the same for the fundamental and for the slot harmonics. We denote this value by β_p. Thus the slot harmonics due to the stator winding distribution are in the stator reference frame

$$b_{k(p+gQ1)} = \frac{\sqrt{2}}{\pi} \frac{\mu_0}{\delta''_{p+gQ1}} \frac{m_1 q_1 N_{1u}}{a_1} \xi_{1(p+gQ1)} \xi_{\epsilon(p+gQ1)} I_1 \frac{p}{p+gQ_1} \cdot \cos[(p+gQ_1)\vartheta_1 - \omega t - \varphi + \beta_p] \quad (69)$$

The addition of k as a subscript indicates harmonics due to the winding distribution.

The origin lying at the centre of a slot, the angle φ_{kQ1} in Eq. (60) is

$$\varphi_{kQ1} = k\pi$$

The flux density harmonics produced by the stator slot openings and the fundamental of the m.m.f. distribution are, in the stator reference frame, according to (62) and (15)

$$b_{u(p+gQ1)} = \frac{1}{2} \hat{b}_p \frac{\hat{\Lambda}_{gQ1}}{\Lambda_o} \cos[(p+gQ_1)\vartheta_1 - \omega t - \varphi_F + \beta_p - g\pi] \quad (70)$$

where k = 1, 2, 3, ... in (62) has been replaced by g = ±1, ±2, ±3, ... The addition of u as a subscript indicates harmonics due to the slotting.

At a fixed point in the air-gap the flux density varies as a sinusoidal function of time, and the flux densities (69) and (70) can be represented by the corresponding phasors $\mathbf{B}_{k(p+gQ1)}$ and $\mathbf{B}_{u(p+gQ1)}$, Fig. 19. The machine operates, in the figure, as a generator with a lagging power factor. As can be seen from the phasor diagram, the flux density

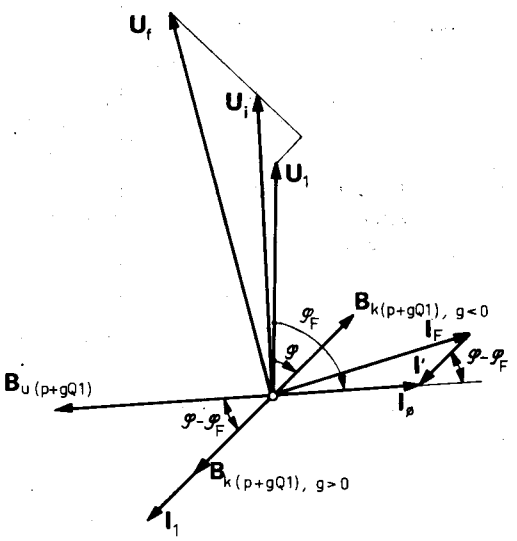

Fig. 19. The phasor diagram of a synchronous machine; $\mathbf{B}_{k(p+gQ1)}$ are slot harmonics due to the winding distribution and $\mathbf{B}_{u(p+gQ1)}$ are harmonics due to the slot openings.

harmonics due to the slotting augment those winding slot harmonics which rotate in the same direction as the fundamental (g > 0) and, depending on the case, either augment or diminish those rotating in the opposite direction (g < 0). At a leading power factor the reverse is true. From the phasor diagram we also see that the phase difference between the flux density harmonics due to the slotting and the slot winding harmonics rotating in the direction of the fundamental equals that between the excitation current component $\mathbf{I}'$ required to compensate the armature reaction and the resulting excitation

current $\mathbf{I}_\phi$. Hence the amplitude of the resulting slot harmonic rotating in the direction of the fundamental is proportional to the field current I_F, independent of the phase of the load current, if only the ratio of the flux density components $b_{k(p+gQ1)}$ and $b_{u(p+gQ1)}$ is correct. By using this flux density harmonic to produce the excitation voltage, self-regulation can be obtained.

If all slots are not open the phase difference between the harmonics due to slot openings and the harmonics due to the winding distribution can be changed by changing the location of open slots. Then the angle φ_μ in the equation of the specific permeance changes. It is thus also possible to obtain self-regulation with harmonics lower than the slot harmonics.

According to Chapter 2 a negatively compounded machine can be changed into a positively compounded one by turning the phase of the excitation current component proportional to load current through 180°, that is by reversing the terminals of the current transformer. As seen from Fig. 19, the phase of the component proportional to the load current changes by 180° if we use the slot harmonic rotating in the direction opposite to that of the fundamental ($g < 0$), and the compound is then positively connected. However, a machine has to be initially designed for either negative or positive compounding and the design cannot be changed in a completed machine because the pole pair number of the auxiliary winding is not the same for negative and positive compounding.

As is evident from the foregoing, several flux density harmonics may be used to obtain self-regulation. Which one of them is most useful is decided by the height of the voltage induced by the harmonic in the rotor auxiliary winding and by the reactance value of the auxiliary winding. These are influenced by the amplitude of the harmonic, by its speed with reference to the rotor and by its wave-length. Furthermore, the wave-length has an effect on how many phases there can be accommodated in the rotor. Moreover, the losses in the auxiliary winding due to the rectifier load depend on the number of phases of the auxiliary winding. These things are studied in the following.

4 RECTIFICATION

4.1 EQUIVALENT RATING

In following an infinite bus is assumed to supply the rectifier implying that the a.c. voltage remains sinusoidal under load. The inductance of the d.c. circuit is assumed to be large enough to preclude fluctuation of the direct current. In the case of the excitation circuit under investigation the first assumption is not strictly valid: the inductance of the auxiliary winding causes the voltage to deviate from sinusoidal waveform when this winding is loaded. In contrast, the inductance of the field winding is large enough to render the second assumption valid in practice.

The current in the a.c. circuit is composed of rectangular sections. The fundamental of this current alone produces power together with a sinusoidal voltage. The harmonics of the current, however, cause losses in the auxiliary winding of the rotor.

Consider the copper loss of the auxiliary winding when the copper area A at disposal for the winding is fixed. Denote the number of phases by m and the number of turns in one phase by N_{At}. The copper area of one conductor is

$$A_j = \frac{A}{2mN_{At}}$$

and the resistance of one phase winding

$$R_A = \frac{N_{At} l_{Am}}{\gamma A_j} = \frac{2l_{Am}}{\gamma A} mN_{At}^2 = K_1 mN_{At}^2 \tag{71}$$

$$K_1 = \frac{2l_{Am}}{\gamma A} \tag{72}$$

where γ is the electrical conductivity of the conductor and l_{Am} the mean length of one turn. The abbreviation K_1 is a constant, independent of the number of phases.

The phase voltage of the auxiliary winding is

$$U_v = K_2 N_{At} \tag{73}$$

where K_2 is a constant, independent of the number of phases.

The copper loss is obtained by the aid of (71) and (73):

$$P_H = mI_v^2 R_A = \frac{K_1}{K_2} (mI_v U_v)^2 \tag{74}$$

where I_v is the r.m.s. value of the phase current. The most favourable rectifier connection, as regards the temperature rise of the auxiliary winding, is that which has the smallest ratio of copper loss to d.c. power. Instead of the numerical value of the loss its square root may be used. Thus, according to (74), for the most favourable connection the ratio

$$K = \frac{mI_v U_v}{I_t U_t} \tag{75}$$

is minimum; I_t is the direct current and U_t the arithmetic mean of the direct voltage. The power mI_vU_v is, in rectifier circuits supplied from a transformer, the equivalent rating of the transformer's secondary winding. In the following the power mI_vU_v is called the equivalent rating of the auxiliary winding.

4.2 *m*-PHASE RECTIFICATION

An *m*-phase half-wave rectifier circuit is shown in Fig. 20. The arithmetic mean of the direct voltage is

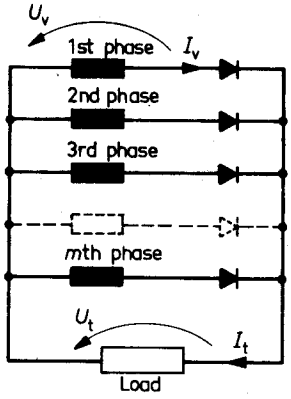

Fig. 20. m-phase half-wave rectification.

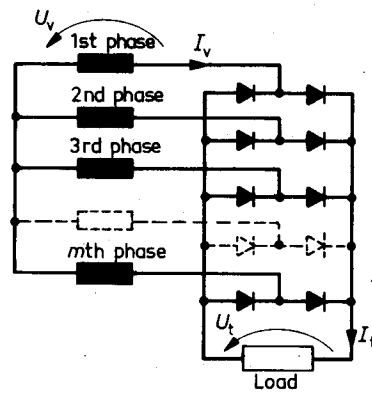

Fig. 21. m-phase full-wave rectification.

$$U_t = \sqrt{2}\,\frac{\sin\frac{\pi}{m}}{\frac{\pi}{m}}\,U_v \tag{76}$$

The r.m.s. value of the phase current is

$$I_v = \frac{I_t}{\sqrt{m}} \tag{77}$$

The ratio of equivalent rating to d.c. power is

$$K = \frac{mU_vI_v}{U_tI_t} = \frac{\pi}{\sqrt{2m\sin\frac{\pi}{m}}} \tag{78}$$

An *m*-phase full-wave rectifier circuit is shown in Fig. 21. When the number of phases is even, the pulses in the direct voltage number m; when the number of phases is odd the pulses number $2m$. The arithmetic mean of the direct voltage is the same in both cases:

$$U_t = 2\sqrt{2}\,\frac{\sin\frac{\pi}{m}}{\frac{\pi}{m}}\,U_v \tag{79}$$

The r.m.s. value of the phase current is

$$I_v = \sqrt{\frac{2}{m}}\,I_t \tag{80}$$

and the ratio of equivalent rating to d.c. power is

$$K = \frac{mU_vI_v}{U_tI_t} = \frac{\pi}{2\sqrt{m}\,\sin\frac{\pi}{m}} \tag{81}$$

Eqs. (78) and (81) are valid for a balanced m-phase winding with its phases spaced by $2\pi/m$ electrical radians. This condition is not true for a two-phase winding. The two-phase winding is in reality a four-phase winding of which phases 1 and 2 are used (Fig. 22 a), or phases 1 and 3 and phases 2 and 4 respectively have been connected in series (Fig. 22 b).

For single-phase full-wave rectification, m in (81) equals 2. This is because the single-phase voltage may be imagined as composed of the difference of two voltages with a phase difference of 180°. In single-phase half-wave rectification the direct current cannot be assumed completely free of pulsation. When the load is a pure resistive load, the ratio of equivalent rating to d.c. power is $\pi^2/(2\sqrt{2}) = 3{,}5$.

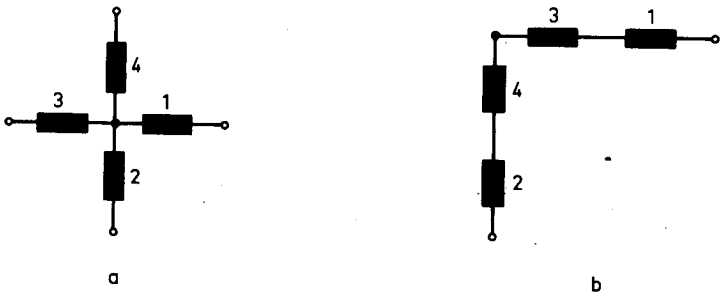

Fig. 22. a) A star-connected four-phase winding. b) A four-phase winding connected to constitute a two-phase winding.

As can be seen from Eqs. (78) and (81), the equivalent rating to d.c. power ratio with half-wave rectification is twice that of the corresponding full-wave rectification. The smallest equivalent rating is required when three-phase full-wave rectification is used (K = 1,05), and it follows that this is the most favourable connection as regards the temperature rise of the auxiliary winding.

4.3 REPLACING THE RECTIFIER LOAD BY AN EQUIVALENT RESISTANCE LOAD

If the alternating voltage is assumed to remain sinusoidal when the rectifier is connected to a load and if the overlap of current is ignored, the alternating voltage and the fundamental of the alternating current are in phase. In studies concerning the fundamental of the current alone the rectifier load may be replaced by an equivalent star-connected resistance load (Fig. 23). The resistance per phase is

$$R' = \frac{U_v}{I_{v1}}$$

where U_v is the phase voltage and I_{v1} the r.m.s. value of the fundamental of the alternating current.

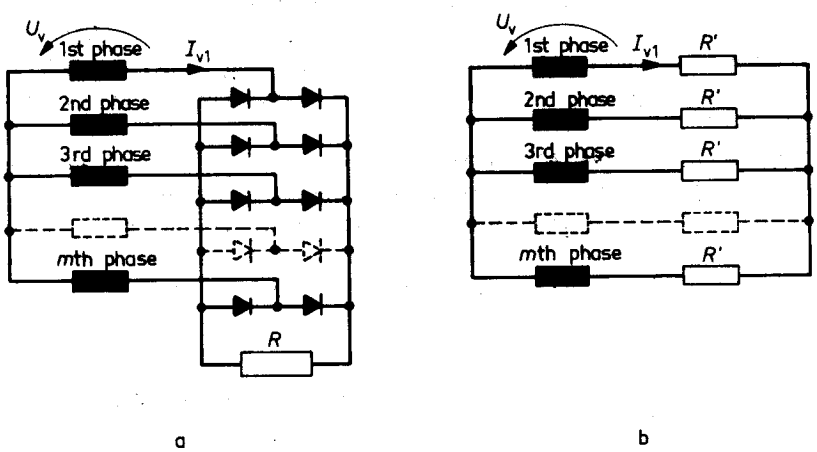

Fig. 23. Replacing a rectifier load (a) by its equivalent resistance (b).

With m-phase half-wave rectification the fundamental a.c. is

$$I_{v1} = \frac{\sqrt{2}}{\pi} I_t \sin \frac{\pi}{m} \tag{82}$$

The equivalent resistance for half-wave rectification is obtained using Eq. (76):

$$R' = \frac{1}{\sqrt{2}} \frac{\frac{\pi}{m}}{\sin \frac{\pi}{m}} \frac{\pi}{\sqrt{2}} \frac{1}{\sin \frac{\pi}{m}} \frac{U_t}{I_t} = \frac{\pi^2}{2m \sin^2 \frac{\pi}{m}} R \tag{83}$$

where R is the load resistance of the d.c. circuit.

With m-phase full-wave rectification the fundamental a.c. is

$$I_{v1} = \frac{2\sqrt{2}}{\pi} I_t \sin \frac{\pi}{m} \tag{84}$$

Using Eq. (79), the equivalent resistance for full-wave rectification is obtained:

$$R' = \frac{1}{2\sqrt{2}} \frac{\frac{\pi}{m}}{\sin\frac{\pi}{m}} \frac{\pi}{2\sqrt{2}} \frac{1}{\sin\frac{\pi}{m}} \frac{U_t}{I_t} = \frac{\pi^2}{8m\sin^2\frac{\pi}{m}} R \tag{85}$$

The a.c. power losses in the equivalent resistance equal the d.c. losses in the true circuit. In the following considerations the rectifier load is replaced by its equivalent resistance.

5 AUXILIARY WINDING OF THE ROTOR

5.1 EQUIVALENT CIRCUIT FOR THE AUXILIARY WINDING

The velocity of the flux density harmonics due to the stator current is not equal to the rotor speed. Therefore the harmonics together with the auxiliary winding in the rotor constitute a wound-rotor induction machine, in which the rotor circuit acts on the rectifier load. The current in the rotor auxiliary winding suppresses harmonics, in the first place all those which have the same number of pole pairs as the auxiliary winding. However, from this no increase of the stator current ensues, nor any change of the rotor speed, as in an induction machine. The magnitude of the stator current is independent of the load of the auxiliary winding. Hence the imagined induction machine is supplied by an ideal current source.

The following basic equations are valid for a slip-ring machine [3, p. 218]:

$$\mathbf{U}_1 = \mathbf{I}_1 \mathbf{Z}_{11} + \mathbf{I}_2 \mathbf{Z}_0$$

$$\mathbf{U}_2 = \mathbf{I}_2 \mathbf{Z}_{22} + s\mathbf{I}_1 \mathbf{Z}_0$$

where $\mathbf{U}_1$ is the stator phase voltage, $\mathbf{U}_2$ the phase voltage between slip-rings, $\mathbf{I}_1$ the stator current, $\mathbf{I}_2$ the rotor current, and s the slip. When the iron loss is ignored, the impedances are

$$\mathbf{Z}_0 = \mathrm{j}X_\mathrm{m} = \text{magnetizing reactance in the saturation state concerned}$$

$$\mathbf{Z}_{11} = R_1 + \mathrm{j}(X_{1\sigma} + X_\mathrm{m}) = \text{no-load impedance from the stator side}$$

$$\mathbf{Z}_{22} = R_2 + \mathrm{j}s(X_{2\sigma} + X_\mathrm{m}) = \text{no-load impedance from the rotor side}$$

The equations are valid when the numbers of phases in the stator and rotor are equal and the numbers of effective turns are equal ($N_{1t}\xi_{1p} = N_{2t}\xi_{2p}$). These presumptions have no effect on the universal applicability of the equations, but they simplify the equations.

When the stator current is constant, the equivalent circuit satisfying the equation for $\mathbf{U}_2$ above, and shown in Fig. 24, is obtained for the rotor circuit. The induced

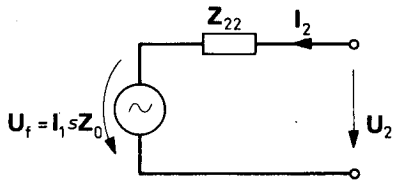

Fig. 24. The equivalent circuit for the rotor circuit of an asynchronous machine.

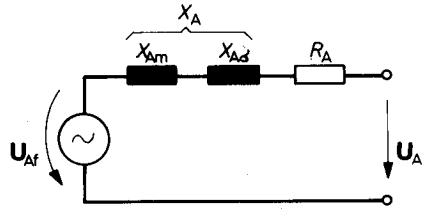

Fig. 25. The equivalent circuit for the auxiliary winding of the rotor.

voltage $\mathbf{U_f = I_1 s Z_o}$ is an ideal voltage source generated by the stator current. The frequency applicable for the reactances is the slip multiplied by the stator frequency, i.e., the frequency in the rotor circuit. Hence the equivalent circuit per phase shown in Fig. 25 is obtained for the auxiliary winding of the rotor. It is the normal equivalent circuit for a synchronous machine, where X_{Am} is the magnetizing reactance, $X_{A\sigma}$ the leakage reactance, X_A the synchronous reactance ($X_A = X_{Am} + X_{A\sigma}$), and R_A the resistance, all values per phase. The flux density harmonic produced by the stator winding induces the voltage U_{Af}.

The auxiliary winding of the rotor may thus be considered like a normal synchronous generator, and in the first place like a non-salient-pole generator. Even if the machine has salient poles, the generator composed of the auxiliary winding in the slots of the pole shoes is most nearly a non-salient-pole machine because the air-gap is constant or almost constant within the area of several consecutive poles, depending on the form of the pole shoe.

5.2 BUILD-UP OF SELF-EXCITATION

When a generator is started up, there is at first in its air-gap a residual flux density, which together with the permeance variations of the air-gap produces a flux density harmonic b_ν. This induces in the auxiliary winding a voltage, which in its turn causes a small field current. If the field current augments the residual flux, the field current supplied by the auxiliary winding increases to a value determined by the saturation and by the impedance of the circuit composed of the auxiliary winding and the field winding.

The small residual voltage acting on the rectifier bridge can be increased by connecting a capacitor C_k, shown in Fig. 26, in parallel with the rectifier bridge (so-called Boucherot circuit). Below the threshold voltage, the resistance of the diodes in the forward direction is nearly infinite. Then the voltage U_o acting on the bridge is

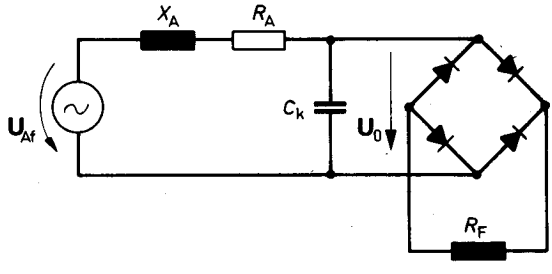

Fig. 26. The rotor circuit with Boucherot capacitor C_k.

$$\mathbf{U_0} = \frac{\mathbf{U_{Af}}}{\mathrm{j}\omega_\nu C_k \left[R_A + \mathrm{j}\left(X_A - \frac{1}{\omega_\nu C_k} \right) \right]} \tag{86}$$

If the resistance of the auxiliary winding is small, and choosing $X_A = 1/(\omega_\nu C_k)$, the voltage U_o according to (86) is high and the diodes become conducting.

The capacitor C_k also has another significance. It reduces the variations of the field current due to changes in the field winding resistance owing to varying temperature. The field current in Fig. 26 is, namely,

$$I_F = K_t \frac{U_{Af}}{\sqrt{[R_A + R'(1 - \omega_\nu C_k X_A)]^2 + (X_A + R_A R' \omega_\nu C_k)^2}} \tag{87}$$

where K_t is the direct current divided by the fundamental phase current for the connection under consideration (in Fig. 26, $K_t = \pi/2\sqrt{2}$) and R' the equivalent resistance of the rectifier load. If $X_A = 1/(\omega_\nu C_k)$ and R_A is small

$$I_F \approx K_t \frac{U_{Af}}{X_A} \tag{88}$$

i.e., the field current is independent of the field winding resistance.

5.3 FIELD CURRENT SUPPLIED BY THE AUXILIARY WINDING

We now consider what current is produced with different harmonics and values of the number of turns N_{At} in the circuit shown in Fig. 25 when the load consists of the equivalent resistance R' of the rectifier load. The winding resistance R_A is imagined to be part of the load resistance R'. Denote the leakage coefficient of the winding by σ_A. The leakage reactance is then

$$X_{A\sigma} = \sigma_A X_{Am}$$

σ_A is assumed to be constant, independent of the harmonic. It is further assumed that the amplitudes of the different flux density harmonics can be made equal. The equivalent air-gap δ''_ν is assumed to be the same for all harmonics.

The circuit under consideration is shown in Fig. 27. The current in the circuit is

$$I = \frac{U_{Af}}{\sqrt{R'^2 + X_A^2}} \tag{89}$$

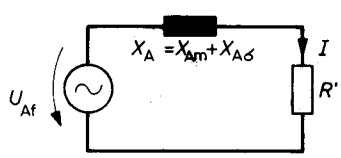

Fig. 27. Simplified equivalent circuit for the excitation circuit.

The induced voltage U_{Af} is [18, p. 209]

$$U_{Af} = \frac{1}{\sqrt{2}} \frac{\omega_\nu}{\nu} N_{At} \xi_{A\nu} DL \hat{b}_\nu \tag{90}$$

where $\xi_{A\nu}$ is the winding factor of the auxiliary winding for the νth harmonic, D the air-gap diameter and L the (effective) length of the rotor core.

The magnetizing reactance of an m-phase winding having ν pole pairs is [18, p. 322]

$$X_{\mathrm{Am}} = \frac{m}{\pi} \frac{\mu_0}{\delta_\nu''} \frac{\omega_\nu}{\nu^2} (N_{\mathrm{At}} \xi_{\mathrm{A}\nu})^2 DL \tag{91}$$

The angular frequency ω_ν in (90) and (91) is

$$\omega_\nu = \left| \left(1 - \frac{\nu}{p}\right) \right| \omega$$

We introduce abbreviations for U_{Af} and X_{A}:

$$U_{\mathrm{Af}} = U_{\mathrm{A1}} N_{\mathrm{At}} \left| \frac{1 - \mathrm{n}}{\mathrm{n}} \right| \tag{92}$$

$$X_{\mathrm{A}} = X_{\mathrm{A1}} N_{\mathrm{At}}^2 \frac{|1 - \mathrm{n}|}{\mathrm{n}^2} \tag{93}$$

where

$$\mathrm{n} = \frac{\nu}{p} \tag{94}$$

$$U_{\mathrm{A1}} = \frac{1}{\sqrt{2}} \frac{\omega}{p} \xi_{\mathrm{A}\nu} DL \hat{b}_\nu \tag{95}$$

$$X_{\mathrm{A1}} = (1 + \sigma_{\mathrm{A}}) \frac{m}{\pi} \frac{\mu_0}{\delta_\nu''} \frac{\omega}{p^2} \xi_{\mathrm{A}\nu}^2 DL \tag{96}$$

Substituting U_{Af} and X_{A} in (89) we get

$$I = \frac{U_{\mathrm{A1}}}{\sqrt{R' X_{\mathrm{A1}}}} \frac{\sqrt{\frac{X_{\mathrm{A1}} N_{\mathrm{At}}^2}{R'}} \left| \frac{1 - \mathrm{n}}{\mathrm{n}} \right|}{\sqrt{1 + \left(\frac{X_{\mathrm{A1}} N_{\mathrm{At}}^2}{R'}\right)^2 \left(\frac{1 - \mathrm{n}}{\mathrm{n}^2}\right)^2}}$$

Denote

$$k = \frac{X_{\mathrm{A1}} N_{\mathrm{At}}^2}{R'} \tag{97}$$

and form the ratio

$$\frac{I}{\frac{U_{\mathrm{A1}}}{\sqrt{R' X_{\mathrm{A1}}}}} = \bar{I} = \frac{\sqrt{k} |\mathrm{n}(1 - \mathrm{n})|}{\sqrt{\mathrm{n}^4 + k^2 (1 - \mathrm{n})^2}} \tag{98}$$

The current is now presented as a dimensionless fraction ($\bar{I}$), which is a function of n and k, which latter k is a function of N_{At} alone. $\bar{I}$ is shown in Fig. 28 as a function of n with k as parameter.

When k is constant, the current has two extremes. One lies in the range $0 < \mathrm{n} < 1$ and the other at a negative value of n. With constant n, the current has an extreme value with regard to k. The extreme points are obtained from the equations

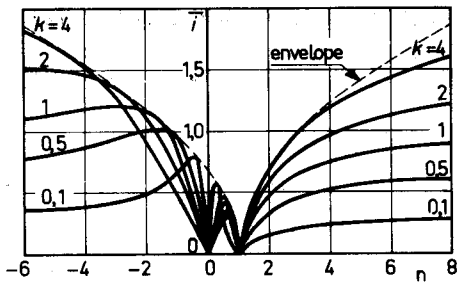

Fig. 28. Eq. (98), $\bar{i} = f(n, k)$, graphically represented.

$$\frac{\partial \bar{i}}{\partial n} = \sqrt{k}\,\frac{(1-2n)[n^4 + k^2(1-n^2)] - n(1-n)[2n^3 - k^2(1-n)]}{\sqrt{[n^4 + k^2(1-n)^2]^3}} = 0$$

$$\frac{\partial \bar{i}}{\partial k} = n(1-n)\,\frac{n^4 + k^2(1-n)^2 - 2k^2(1-n)^2}{2\sqrt{k}\,\sqrt{[n^4 + k^2(1-n)^2]^3}} = 0$$

or simplified

$$\frac{n^4}{k^2} = (1-n)^3 \tag{99}$$

$$k^2 = \frac{n^4}{(1-n)^2} \tag{100}$$

For simplicity the absolute value signs are omitted, since they have no effect on the location of the extreme but only the type of extreme value. The solution of the set of equations (99), (100) is

$$\begin{cases} n = 0 \\ k = 0 \end{cases}$$

This is not, however, the solution for the zero points of the partial derivates because the denominator of the derivates becomes zero at these values. Therefore the current has no extreme as a function of the two variables n and k. From (99) we may determine the value of n which gives the current its extreme value when k is constant. The solution cannot be explicitly written. With constant n the value of k at which the current attains its extreme value can be solved from (100):

$$k = \frac{n^2}{|1-n|}$$

On the other hand, according to (97) and (93),

$$k = \frac{X_{A1} N_{A1}^2}{R'} = \frac{n^2}{|1-n|}\,\frac{X_A}{R'}$$

It follows that at the extreme point of the current X_A must equal R'. The points satisfying this condition are located, in Fig. 28, on the envelope of the family of curves.

The magnitude of the current is then

$$\frac{I}{\frac{U_{A1}}{\sqrt{R'X_{A1}}}} = \sqrt{\frac{|1-n|}{2}} \tag{101}$$

As can be seen from this, and also from Fig. 28, the current increases infinitely when n approaches infinity.

Hence, if we disregard the amplitude of the harmonic, the highest field current is obtained by designing the auxiliary winding for the highest possible harmonic order. When the amplitude of the flux density harmonic is taken into account, the first slot harmonic is obviously the most advantageous. The first harmonics may be of the same order of magnitude in amplitude as the first slot harmonics and even higher. As can be seen from Eq. (101), the amplitudes of the first harmonics should, however, be much higher than those of the slot harmonics in order that the first harmonics could maintain higher field currents than the slot harmonics.

If the auxiliary winding cannot maintain a sufficient field current, the reactance of the auxiliary winding can be wholly or partly compensated by connecting a capacitor in series with each phase winding of the auxiliary winding. Then the highest field current is generated by the harmonic inducing the highest voltage U_{Af}. According to Eqs. (92), (95), (55) and (17), U_{Af} is proportional to the product

$$U_{Af} \sim \frac{\xi_\nu}{|n|}\left(\left|\frac{1}{n} - 1\right|\right)$$

When $|n| \geqslant 5$, $|1/n - 1| = 0{,}85 \cdots 1{,}2$ i.e. $|1/n - 1|$ varies rather little, whereas $\xi_\nu/|n|$ varies greatly with different harmonics, depending on the winding technique. Particularly for the first slot harmonics $\xi_\nu/|n|$ is high. For lower harmonics an appropriate winding design (high ξ_ν) enables $\xi_\nu/|n|$ to be made equal in magnitude with the first slot harmonics and even higher. The first slot harmonic is, however, more favourable in that owing to the higher frequency smaller capacitors are required than for the lower harmonics.

In the case of the Boucherot circuit (Fig. 26) the equation (88) is valid for the field current at resonance. The highest field current is then obtained with the harmonic for which U_{Af}/X_A is highest. For harmonics with equal amplitudes U_{Af}/X_A is, according to (92) and (93), the greater the higher harmonic under consideration. Hence when the amplitudes of the harmonics are also taken into account, the first slot harmonic is the most advantageous also in the Boucherot circuit.

5.4 DESIGN CONSIDERATIONS

Synchronous generators are usually provided with a damper winding. In a machine excited by harmonics the damper winding must be devised so as to cause no suppression of the harmonic (ν) utilized for excitation. The number of slots of the damper winding then has to be

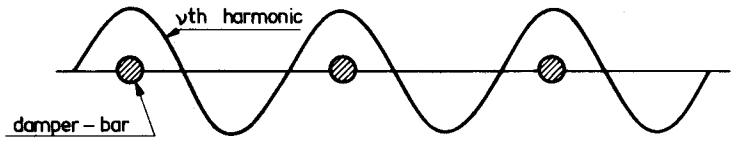

Fig. 29. A damper winding, which does not suppress the νth harmonic.

$$Q = \frac{\nu}{k}$$

where k is an integer. The νth harmonic then always induces in all bars of the damper winding a voltage having the same phase and the same magnitude (Fig. 29), whereby no damping current is produced. The slot pitch of the damper winding will then be multiple of the slot pitch of the auxiliary winding. It follows that the damper winding may be placed in the same slots with the auxiliary winding. If the auxiliary winding is designed for the first slot harmonic, the highest possible slot number of the damper winding is

$$Q = Q_1 + p$$

If the auxiliary winding is made for lower harmonics, then the slot number of the damper winding will be small. For instance for the 5th harmonic the highest possible number of slots of the damper winding would be $5p$ while the normal slot number is $(10\cdots20)p$. This causes poor characteristics of the damper winding.

The harmonics due to the stator winding distribution induce in the stator winding a voltage of the fundamental frequency. The slot openings of the stator too, or more generally the irregularities of the stator surface, give together with the air-gap m.m.f. rise to flux density harmonics having the fundamental frequency in the stator coordinates. Hence the harmonic used for excitation causes no harmonics in the voltage waveform. However, the stator slot openings influence the harmonic voltages induced in the stator winding by the rotor harmonics. These voltages are not of the fundamental frequency. The stator slot openings strengthen in particular the harmonics with a pole pair number equal to that of the stator slot harmonics. There are many means to suppress harmonics in the voltage curve [20, p. 530]. Skewing the slots of the damper winding by one stator slot pitch eliminates the first slot harmonic from the voltage curve. A skewness equivalent to half of the slot pitch eliminates the second slot harmonic, and so on. The same effect is obtained by skewing the pole shoes. These means cannot be efficiently utilized in the excitation circuit under consideration if the auxiliary winding is made for the first slot harmonic, because skewing by one stator slot pitch makes the winding factor of the auxiliary winding to be zero for the first slot harmonic. Using a small skewness, however, the higher slot harmonics may be suppressed to a certain extent.

The same effect as with skewing may be obtained by displacing the N poles by 1/4 stator slot pitch in one direction and the S poles by the same distance in the other. This method is also appropriate for a machine excited by the first slot harmonic. Then the phase difference between the voltages induced in the auxiliary windings located in adjacent poles is 90°. The auxiliary winding may therefore be made as a two-phase

winding, one phase winding consisting of the single-phase windings located in the N poles and the other phase winding consisting of those in the S poles. However, the second slot harmonic cannot be eliminated by this method. On the other hand, the higher harmonics are usually small enough to have a negligible disturbing effect.

A highly effective means to suppress the slot harmonics in the voltage curve is to use an appropriate fractional-slot winding in the stator. This method is also applicable in a generator excited by harmonics. The first slot harmonic, and with a pole pair number of the generator in excess of two also higher slot harmonics, can always be suppressed by using a proper fractional-slot winding.

When the generator falls out of step the fundamental of the flux density distribution moves with respect to the rotor. Also with unbalanced load a flux density wave having a wave-length equal to that of the fundamental is encountered, but which rotates in the opposite direction. These waves should not, however, induce in the auxiliary winding any voltage which might impose a dangerous overvoltage on the rectifier. Connecting the coils of the auxiliary winding in series within the range of two pole pairs precludes the occurrence of such voltages. This is seen as follows.

Denote the coil sides of the auxiliary winding located in the range of two consecutive poles of the machine by running numbers 1···k (Fig. 30). The geometric angle between

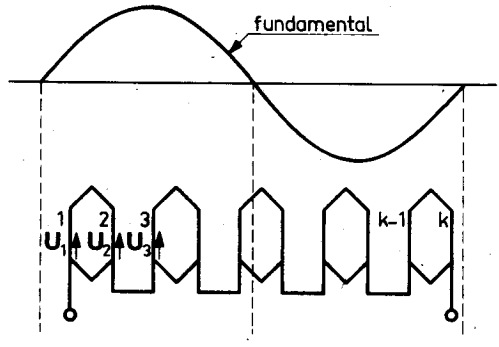

Fig. 30. Voltages induced in the coil sides of the auxiliary winding by the fundamental of the flux density wave.

the coil sides is π/ν, where ν is the number of pole pairs of the auxiliary winding. The fundamental flux density wave induces in the coil sides the voltages

$$\mathbf{U}_1 = \mathbf{U}_1$$
$$\mathbf{U}_2 = \mathbf{U}_1\, e^{-jp\pi/\nu}$$
$$\mathbf{U}_3 = \mathbf{U}_1\, e^{-j2p\pi/\nu}$$
$$\vdots$$
$$\mathbf{U}_k = \mathbf{U}_1^{-j(k-1)p\pi/\nu} = \mathbf{U}_1\, e^{-j(2\nu/p-1)p\pi/\nu}$$

In the series connection the sum of the induced voltages is

$$\mathbf{U} = \mathbf{U}_1 - \mathbf{U}_2 + \mathbf{U}_3 \pm \cdots - \mathbf{U}_k = \mathbf{U}_1(1 - e^{-jp\pi/\nu} + e^{-j2p\pi/\nu} \pm \ldots - e^{-j(2\nu/p-1)p\pi/\nu}) \quad (102)$$

The expression (102) is a geometrical series having the sum

$$\mathbf{U} = \mathbf{U}_1 \frac{1 - e^{-j2\pi}}{1 + e^{-jp\pi/\nu}} = 0$$

since the numerator is always zero.

A fractional-slot winding may produce subharmonics, for which the inverse value of the order, i.e. p/ν, is an odd integer. For these the sum of the series (102) is not zero but kU_1, as is easily seen from Eq. (102). However, the subharmonics are not suitable for producing the excitation voltage, as was observed in Chapter 3.3.1.

If parallel paths are provided in the auxiliary winding, then each path must have ν/p coil groups in series in order that the fundamental at unbalanced load, or when the machine falls out of step, might not induce a voltage in the auxiliary winding. Hence the greatest number of the parallel paths is p.

Summary. It has been shown that several harmonics may be used to produce the excitation voltage. The highest harmonic which is practical is obviously the first slot harmonic, since for higher ones the pole pitch of the harmonics is so small as to render the making of the auxiliary winding highly difficult. The slot harmonics are more favourable than the lower harmonics in that, as has been shown previously, the auxiliary winding is able to supply a higher current with the slot harmonics than with lower harmonics. Then, if the harmonic used for excitation is not strong enough in a generator of standard construction, the requisite artificial augmentation of the slot harmonics is at a minimum. Secondly, when slot harmonics are used all stator slot openings are equal, while in the case of lower harmonics being used part of the slots must be closed, or other means must be used to achieve the desired permeance variation. Considering the damper winding, the slot harmonics are more advantageous in that with them it is possible to make the number of damper bars equal to that of conventional generators. In contrast, for the lower harmonics the number of damper bars remains rather small. As regards suppression of the slot harmonics in the stator voltage waveform, the lower harmonics are superior to the slot harmonics because when the slot harmonics are used the slots of the rotor cannot be efficiently skewed, which is one of the most common procedures. With lower harmonics also this method may be used. On the other hand, an appropriate fractional slot winding may always be used to eliminate the first slot harmonic from the stator voltage waveform also when the excitation voltage is induced by the slot harmonics.

6 LOAD CHARACTERISTICS

6.1 FIELD CURRENT

In the following an expression of the field current is derived, in terms of the air-gap voltage (U_i) and the load of the generator when the auxiliary winding is made for the first slot harmonic.

The equivalent circuit for the excitation circuit is as shown in Fig. 31 when a capacitor C is used to compensate part of the reactance of the auxiliary winding and another capacitor C_k is used to assure the build-up and to eliminate the effects of the field resistance variations. From Fig. 31 the field current is

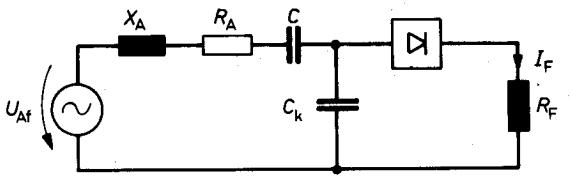

Fig. 31. The equivalent circuit for the excitation circuit.

$$I_F = K_t \frac{U_{Af}}{\sqrt{[R_A + R'(1 - \omega_\nu C_k X_A + C_k/C)]^2 + [X_A - 1/(\omega_\nu C) + R_A R' \omega_\nu C_k]^2}} = K_t \frac{U_{Af}}{Z_F} \tag{103}$$

where

$$Z_F = \sqrt{[R_A + R'(1 - \omega_\nu C_k X_A + C_k/C)]^2 + [X_A - 1/(\omega_\nu C) + R_A R' \omega_\nu C_k]^2} \tag{104}$$

U_{Af} is calculated from (90), where $\hat{b}_\nu$ is composed of the component proportional to the fundamental flux density wave and of that proportional to the stator current. According to (70), the former is

$$\hat{b}_{u(p+Q1)} = \frac{1}{2} \hat{b}_p \frac{\hat{\Lambda}_{Q1}}{\Lambda_o} \tag{105}$$

The air-gap voltage induced by the resulting flux is [18, p. 209]

$$U_i = \frac{\omega}{\sqrt{2}} \frac{DL}{p} \xi_{1p} N_{1t} \hat{b}_p \tag{106}$$

Substituting $\hat{b}_{u(p+Q1)}$ (105) and from (106) $\hat{b}_p$ in (90) gives a voltage component U_{Afu} proportional to the fundamental flux density wave:

$$U_{Afu} = \frac{1}{2}\frac{Q_1}{p+Q_1}\frac{\xi_{A(p+Q1)}N_{At}}{\xi_{1p}N_{1t}}\frac{\hat{\Lambda}_{Q1}}{\Lambda_0}U_i = C_1 U_i \tag{107}$$

$$C_1 = \frac{1}{2}\frac{Q_1}{p+Q_1}\frac{\xi_{A(p+Q1)}N_{At}}{\xi_{1p}N_{1t}}\frac{\hat{\Lambda}_{Q1}}{\Lambda_0} \tag{108}$$

The amplitude of the slot harmonic proportional to the stator current is according to (69)

$$\hat{b}_{k(p+Q1)} = \frac{\sqrt{2}}{\pi}\frac{\mu_0}{\delta''_{p+Q1}}\frac{m_1 q_1 N_{1u}}{a_1}\xi_{1(p+Q1)}\xi_{\epsilon(p+Q1)}\frac{p}{p+Q_1}I_1 \tag{109}$$

Substituting $\hat{b}_{k(p+Q1)}$ in (90) gives a voltage component U_{Afk} proportional to the load current:

$$U_{Afk} = \frac{\mu_0}{\pi}\frac{Q_1\omega}{(p+Q_1)^2}\frac{1}{\delta''_{p+Q1}}\xi_{A(p+Q1)}\xi_{\epsilon(p+Q1)}\xi_{1(p+Q1)}N_{At}\frac{m_1 q_1 N_{1u}}{a_1}DLI_1 = C_2 I_1 \tag{110}$$

$$C_2 = \frac{\mu_0}{\pi}\frac{Q_1\omega}{(p+Q_1)^2}\frac{1}{\delta''_{p+Q1}}\xi_{A(p+Q1)}\xi_{\epsilon(p+Q1)}\xi_{1(p+Q1)}N_{At}\frac{m_1 q_1 N_{1u}}{a_1}DL \tag{111}$$

Denote the stator current component along $\mathbf{U}_i$ by $\mathbf{I}_{1a}$ and the component at right angles to $\mathbf{U}_i$ by $\mathbf{I}_{1r}$ (Fig. 32). $\mathbf{I}_{1r}$ generates in the auxiliary winding a voltage component in

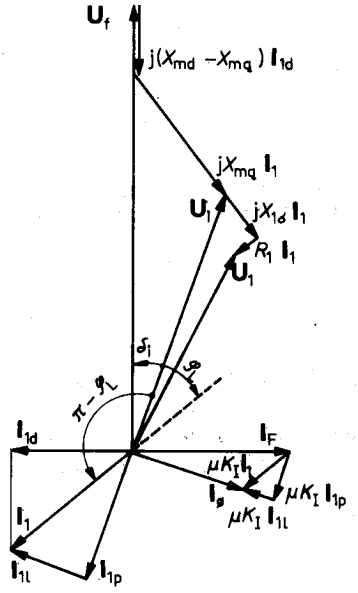

Fig. 32. The phasor diagram of a salient-pole synchronous machine.

phase with $\mathbf{U}_{Afu}$, and $\mathbf{I}_{1a}$ generates a voltage component perpendicular thereto. U_{Af} is therefore

$$U_{Af} = \sqrt{(C_1 U_i + C_2 I_{1r})^2 + (C_2 I_{1a})^2} \tag{112}$$

Substituting (112) in (103) gives

$$I_F = \sqrt{\left(\frac{K_t C_1}{Z_F} U_i + K_I \mu I_{1r}\right)^2 + (K_I \mu I_{1a})^2} \tag{113}$$

where

$$K_I = \frac{K_t C_2}{\mu Z_F} \tag{114}$$

μ is a reduction factor, which is for a non-salient-pole machine [18, p. 366]

$$\mu = \frac{m_1}{\sqrt{2}} \frac{\xi_{1p} N_{1t}}{\xi_{Fp} N_{Ft}} \tag{115}$$

where ξ_{Fp} is the winding factor of the field winding for the fundamental and N_{Ft} the number of turns of the field winding in series. The factor μ does not affect I_F because the same terms in the expression of the field current have been multiplied and divided by it. The value of K_I is only reduced by μ to have a more practical magnitude, as it will be found later.

The phasor diagram of the excitation circuit has also been shown in Fig. 32. The component I_ϕ of the field current is

$$I_\phi = \frac{K_t C_1}{Z_F} U_i \tag{116}$$

If, at changing load, the field current is regulated so that I_ϕ remains constant, then the air-gap voltage U_i, which is proportional to I_ϕ, also remains constant. The change of the field current then compensates the effect of the armature reaction and the field current component proportional to the load current is

$$I' = \mu I_1 \tag{117}$$

i.e., the factor K_I in Eq. (113) must be 1. Owing to the changes of the voltage drops in the stator leakage reactance and resistance, the field current must be regulated (at a lagging power factor) in excess of what the equation (117) indicates. Hence, in order that the terminal voltage might be constant, K_I must be >1. The factor corresponding to K_I in a conventional compound generator is called the compound factor.

Denote the load impedance of the generator per phase with

$$\mathbf{Z}_L = Z_L \angle \varphi_L \tag{118}$$

which contains the stator resistance and the leakage reactance of the generator. Then

$$I_{1a} = \frac{U_i \cos(\pi - \varphi_L)}{Z_L} = -\frac{U_i \cos\varphi_L}{Z_L} \tag{119}$$

$$I_{1r} = \frac{U_i \sin(\pi - \varphi_L)}{Z_L} = \frac{U_i \sin\varphi_L}{Z_L} \tag{120}$$

Substituting (119) and (120) in (113),

$$I_F = U_i \sqrt{\left(\frac{K_t C_1}{Z_F} + \mu K_I \frac{\sin\varphi_L}{Z_L}\right)^2 + \left(\mu K_I \frac{\cos\varphi_L}{Z_L}\right)^2} = G U_i \tag{121}$$

where

$$G = \sqrt{\left(\frac{K_t C_1}{Z_F} + \mu K_I \frac{\sin\varphi_L}{Z_L}\right)^2 + \left(\mu K_I \frac{\cos\varphi_L}{Z_L}\right)^2} \tag{122}$$

Eq. (121) represents the relation between the field current I_F, the air-gap voltage U_i and the load impedance $Z_L \underline{/\varphi_L}$.

6.2 VOLTAGE EQUATIONS OF A SYNCHRONOUS GENERATOR

When determing the operating point of the generator the magnetic saturation must be taken into account, since the internal operating point is determined by the intersection of the magnetization characteristic and the "impedance line" of the excitation circuit similarly as in a d.c. shunt generator, as will be seen later. For simplifying the calculations we assume that the rotor is not saturated by its leakage flux, in which case the magnetizing reactance can be calculated by the aid of the magnetization characteristic from the equation

$$X_{md} = \mu \frac{U_i}{I_\phi} \tag{123}$$

where the point (U_i, I_ϕ) of the magnetization curve is the internal operating point of the machine.

The voltage equations of the synchronous machine in a steady-state condition are [18, p. 396]

$$\mathbf{U}_1 = (R_1 + jX_{1\sigma})\mathbf{I}_1 + jX_{mq}\mathbf{I}_1 + j(X_{md} - X_{mq})\mathbf{I}_{1d} + \mathbf{U}_f \tag{124}$$

$$\mathbf{U}_i = \mathbf{U}_1 - (R_1 + jX_{1\sigma})\mathbf{I}_1 = jX_{mq}\mathbf{I}_1 + j(X_{md} - X_{mq})\mathbf{I}_{1d} + \mathbf{U}_f \tag{125}$$

$$U_f = \frac{X_{md}}{\mu} I_F \tag{126}$$

where X_{mq} is the quadrature-axis magnetizing reactance and I_{1d} the direct-axis component of the stator current. Fig. 32 represents the phasor diagram corresponding to Eq. (124). The phase difference of $\mathbf{U}_f$ with respect to $\mathbf{U}_i$ is denoted by δ_i.

Dividing the voltage equation (125) into two components, one along $\mathbf{U}_i$ and the other perpendicular to $\mathbf{U}_i$, we have

$$\mathbf{I}_1 = I_{1a} + jI_{1r} \tag{127}$$

$$\begin{aligned}\mathbf{I}_{1d} &= (I_{1a}\sin\delta_i - I_{1r}\cos\delta_i)e^{j(\delta_i - \pi/2)} \\ &= I_{1a}\sin^2\delta_i - I_{1r}\sin\delta_i\cos\delta_i - j(I_{1a}\sin\delta_i\cos\delta_i - I_{1r}\cos^2\delta_i)\end{aligned} \tag{128}$$

Substituting (127) and (128) in (125) gives in the component presentation

$$U_i = (X_{md} - X_{mq})\sin\delta_i\cos\delta_i I_{1a} - (X_{md}\cos^2\delta_i + X_{mq}\sin^2\delta_i)I_{1r} + \frac{X_{md}}{\mu}\cos\delta_i I_F \tag{129}$$

$$0 = (X_{md}\sin^2\delta_i + X_{mq}\cos^2\delta_i)I_{1a} - (X_{md} - X_{mq})\sin\delta_i\cos\delta_i I_{1r} + \frac{X_{md}}{\mu}\sin\delta_i I_F \tag{130}$$

I_{1a}, I_{1r}, I_F and U_i can be eliminated from the set of equations (119), (120), (129) and (130) and the angle δ_i can be determined. The result is

$$\delta_i = \arctan \frac{X_{mq} \cos \varphi_L}{Z_L + X_{mq} \sin \varphi_L} \tag{131}$$

6.3 DIRECT-AXIS MAGNETIZING REACTANCE

The direct-axis magnetizing reactance X_{md} can be calculated by the aid of the magnetization curve from Eq. (123). On the other hand, X_{md} corresponding to a definite load impedance $\mathbf{Z}_L$ can be determined by eliminating I_{1a}, I_{1r}, I_F and U_i from the set of equations (119), (120), (121) and (129). The result is

$$X_{md} = \frac{Z_L - (\sin \delta_i \cos \delta_i \cos \varphi_L - \sin^2 \delta_i \sin \varphi_L) X_{mq}}{\frac{Z_L G}{\mu} \cos \delta_i - \sin \delta_i \cos \delta_i \cos \varphi_L - \cos^2 \delta_i \sin \varphi_L} \tag{132}$$

For a non-salient-pole machine $X_{md} = X_{mq} = X_m$, and from (132)

$$X_m = \frac{Z_L}{\frac{Z_L G}{\mu} \cos \delta_i - \sin \varphi_L} \tag{133}$$

6.4 TERMINAL VOLTAGE

The terminal voltage of the generator when used as an isolated generator may be calculated in broad outline as follows:

1. Calculate C_1 (108), C_2 (111) and K_I (114).
2. Calculate G (122) corresponding to the given load.
3. Calculate δ_i (131). For a salient-pole machine X_{mq} may be assumed to be constant, independent of the saturation, since the reluctance of the magnetic circuit in the quadrature axis is determined by the air-gap. For a non-salient-pole machine $X_{mq} = X_{md} = X_m$, and the saturation has to be taken into account as presented in 4 below.
4. Calculate, for a salient-pole machine, X_{md} from (132) or for a non-salient-pole machine, X_m from (133). For the non-salient-pole machine X_m must be iterated to satisfy simultaneously the equations (131) for δ_i and (133) for X_m.
5. Find the point (U_i, I_ϕ) on the magnetization curve satisfying (123), i.e., find the intersection of the magnetization curve and the straight line (123).
6. Calculate I_{1a} (119) and I_{1r} (120).
7. Calculate the terminal voltage U_1 from the equation

$$\mathbf{U}_1 = U_i + (R_1 + \mathrm{j} X_{1\sigma})(I_{1a} + \mathrm{j} I_{1r}) \tag{134}$$

The quantities C_1, C_2, K_I and G calculated in items 1 and 2 are functions of the saturation. It was stated in Chapter 3.3.4.1 that the saturation does not have any great effect on the slot harmonics and hence on the factor C_1. In contrast the saturation effects the lower harmonics through a change of Carter's coefficient. When these

harmonics are used for producing the excitation voltage, C_1 is a function of the saturation. It will be shown later in connection with measurements (Chapter 8.2.3), that also with the slot harmonics C_1 depends to some degree on the saturation, while it is true that the linear range extends far into the saturation range.

C_2 is, according to Eq. (111) inversely proportional to the equivalent air-gap δ''_ν. In the case of the first slot harmonic and of higher harmonics the flux passes only a short distance through iron and the air-gap constitutes the major part of the magnetic circuit. A single-phase winding for the first slot harmonic and its flux pattern are schematically shown in Fig. 33. The pole pitch of the first slot harmonic is approximately half of the

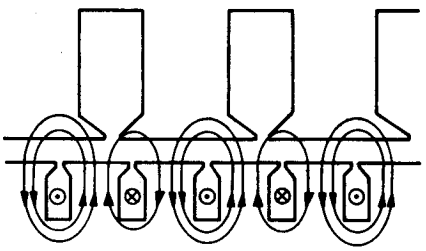

Fig. 33. The flux pattern produced by the rotor auxiliary winding made for the first slot harmonic.

stator tooth pitch. As a consequence the flux of the slot harmonic is not compelled to make the circuit of the stator slot: its path may close through the tooth end. The part of the magnetic circuit subject to saturation consists of the rotor teeth. The saturation of the rotor teeth is determined by the fundamental of the flux density distribution. The teeth coinciding with the crest value of the air-gap flux density are most strongly saturated. According to measurements (Chapter 8.2.2) δ''_ν can be roughly calculated from the equation

$$\delta''_\nu \approx \frac{\hat{v}_\delta + \hat{v}_{z2}}{\hat{v}_\delta} k_c \delta \tag{135}$$

where $\hat{v}_\delta$ and $\hat{v}_{z2}$ are the air-gap m.m.f. and the rotor-tooth m.m.f., respectively, at the crest value of the flux density. For harmonics lower than the slot harmonics the sum of the stator and rotor tooth m.m.f.'s and the stator and rotor yoke m.m.f.'s must be substituted for $\hat{v}_{z2}$ in (135).

The compound factor K_I (114) is proportional to the ratio C_2/Z_F. The terms of Z_F depending on the saturation are the magnetizing and the harmonic leakage reactance of the auxiliary winding. Both are inversely proportional to δ''_ν. If the Boucherot circuit presented in Chapter 5.2 is used, $Z_F \approx X_A$. Because the leakage part of X_A (except the harmonic leakage reactance) is independent of the saturation, X_A decreases somewhat slower than C_2 with increasing saturation. There is then some decrease of C_2/Z_F with increasing saturation.

The terms of G (122) depending on the saturation are K_I and the ratio C_1/Z_F. According to the foregoing, C_1 increases a little and Z_F decreases with increasing saturation. Accordingly C_1/Z_F increases with increasing saturation. It follows that the field current component (I_ϕ) proportional to U_i increases with increasing saturation and

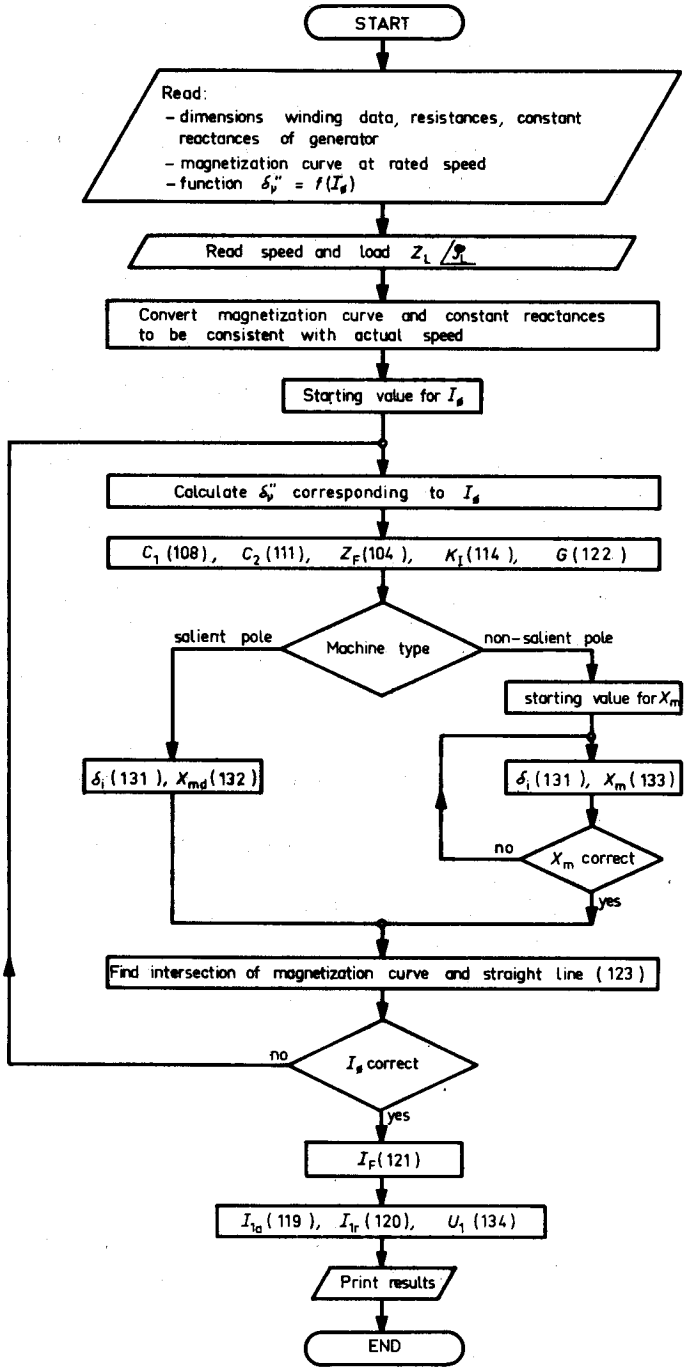

Fig. 34. Calculation of the generator's terminal voltage at a given load.

decreases with decreasing saturation. This is an undesired feature in view of a constant terminal voltage. On the other hand, as has been stated before, C_2/Z_F and K_I, which is proportional to it, decrease with increasing saturation. The field current component ($\mu K_I I_1$) proportional to the load current therefore increases more slowly than directly proportionally to the load current if the saturation (U_i) shows a tendency to rise. This is a favourable feature in view of a constant voltage; it partly compensates the effect exerted on the terminal voltage by the change of C_1/Z_F.

Taking into account the dependence of the equivalent air-gap δ_ν'' on the saturation, the terminal voltage in separate duty can be calculated in accordance with the diagram shown in Fig. 34.

6.5 EFFECT OF SPEED CHANGE ON THE TERMINAL VOLTAGE

In the foregoing the characteristics of the excitation arrangement were studied assuming a constant speed. If the network is small, e.g. a stand-by network, there is some variation of speed at load changes. The power control of prime movers is usually based on changing the speed.

Depending on the nature of the load, different voltage characteristics of the generator are desired. If mainly an active load is concerned, such as lighting load, the voltage should be constant, independent of the frequency. With a reactive load, especially with an asynchronous motor load, the voltage/frequency ratio is often desired to remain constant. Then the flux of the motor and its maximum torque remain constant at varying speed.

The terminal voltage of the generator under investigation with different speeds and loads can be determined by the computation method presented in Chapter 6.4. It is only necessary in the calculations to take observe that the factor C_2 and the reactances are directly proportional to the frequency. Furthermore, the magnetization curve must be reduced to be consistent with the new speed. These changes have been taken into account in the diagram shown in Fig. 34. In the following the no-load voltage is considered as a function of the speed.

At no-load, Z_L in infinite and G (122), δ_i (131), and X_m (132) or (133) are

$$G = \frac{K_t C_1}{Z_F} \tag{136}$$

$$\delta_i = 0 \tag{137}$$

$$X_{md} = X_m = \frac{\mu}{G} \tag{138}$$

The no-load voltage is found as the intersection of the straight line (123) and the magnetization curve. Equating the right-hand sides of Eqs. (123) and (138) we get

$$U_i = \frac{I_\phi}{G}$$

Substituting G (136) and taking into account that the terminal voltage U_1 equals U_i at no-load:

$$U_1 = U_i = \frac{Z_F}{K_t C_1} I_\phi \tag{139}$$

The relation between the no-load voltage and the speed depends on the properties of Z_F. The following extremes are possible:

1. $Z_F \approx$ constant. This is possible if the main terms of Z_F are the resistances. The reactance X_A of the auxiliary winding is then compensated by a capacitor C (Fig. 31). The compensation is complete ($X_A = 1/(\omega_p C)$) at a given speed, whence follows that Z_F can only be constant within a given speed range. When Z_F is constant, the straight line (139) is independent of the speed (in Fig. 35 the straight line (1)). The operating point becomes unstable at the speed at which the straight line (1) coincides with the initial linear part of the magnetization curve. In Fig. 35 the minimum point is denoted by M_1. The no-load voltage varies slightly more strongly than directly proportionally to the speed, curve a in Fig. 36.

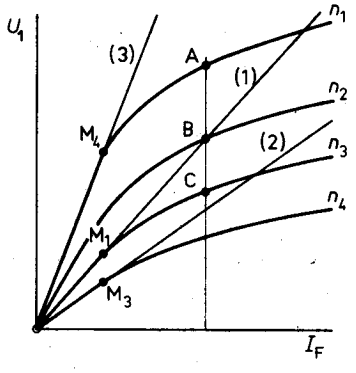

Fig. 35. Magnetization curves at different speeds, $n_1 > n_2 > n_3 > n_4$. Determining the no-load voltage.

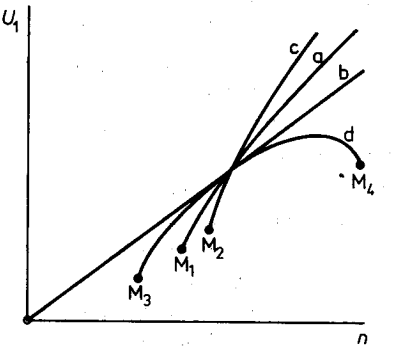

Fig. 36. No-load voltage (U_1) *vs.* speed (n): a) $Z_F \approx$ constant, b) $Z_F \sim n$, c) $Z_F \sim 1/n$, and d) the excitation circuit in accordance with Fig. 31.

2. Z_F is proportional to the speed if the reactance of the auxiliary winding is the main term of Z_F. Because the slope of the line (139) and the magnetization curve are both directly proportional to the speed, the intersections (in Fig. 35 points A, B, and C) all occur at the same value of the field current. The no-load voltage is then directly proportional to the speed, curve b in Fig. 36.
3. Z_F is inversely proportional to the speed if the capacitor C is the main term of Z_F. With increasing speed the slope of the line (139) decreases, so that the no-load voltage increases faster than in case 1, where the slope was constant. In analogy, the voltage decreases faster with decreasing speed than in case 1, curve c in Fig. 36. The unstable point (M_2) now occurs at a higher speed than in case 1.

We shall now consider the kind of no-load properties inherent in the circuit of Fig. 31. In order that the temperature sensitivity might be low, the resistance of the auxiliary winding should be small, as has been said before. The variations of the field winding resistance are eliminated by the capacitor C_k. When R_A is small, Z_F is according to (104)

$$Z_F = \sqrt{[R'(1 - \omega_\nu C_k X_A + C_k/C)]^2 + [X_A - 1/(\omega_\nu C)]^2} \qquad (140)$$

In order that the variations of R' might be eliminated, there must be at rated speed

$$1 - \omega_\nu C_k X_A + C_k/C = 0 \qquad (141)$$

whence

$$Z_F = X_A - \frac{1}{\omega_\nu C} \qquad (142)$$

Since $X_A > 1/(\omega_\nu C)$ (Eq. (141) is not valid otherwise), Z_F is approximately directly proportional to the speed close to the nominal operating point. Then also the no-load voltage is directly proportional to the speed.

With decreasing speed the first term of the square root expression (140) increases. Then Z_F decreases slower than directly proportionally to the speed. At a given speed the line (139) coincides with the initial linear part of the magnetization curve (line (2) in Fig. 35), whereby the operation becomes unstable. The minimum point is denoted by M_3 in Figs. 35 and 36.

When the speed exceeds the resonance speed determined by Eq. (141), the first term of the square root expression (140) increases. Z_F then increases faster than directly proportionally to the speed. At a high enough speed the line (139) coincides with the initial linear part of the magnetization curve (line (3) in Fig. 35). The operation becomes unstable at the point M_4.

Close to the point M_4 there exists a range where the no-load voltage is nearly constant. The excitation circuit can be designed so that the nominal operating point lies within this range. It is true, though, that we are then at a distance from the resonance point (141), in which case the variations of the resistance are not eliminated.

If the power factor of the load is constant (e.g. with a lighting load), the voltage can be made sufficiently constant by choosing a proper compound factor. If the speed is constant and the compound factor is high enough the terminal voltage increases at resistive and reactive load when the load increases. On the other hand the increasing load causes lowering of the speed by a few per cent. Then at the resonance point (141) the no-load voltage decreases. The fall of voltage may then be compensated by means of a proper compound factor.

A transient state precedes the above-considered steady-state condition following a load change. The harmonic excitation circuit under investigation has the character of a compound scheme and it is expected to act like a compound scheme in transient states. This was also found to be true in measurements (Chapter 8.3.3). Since an ample literature exists concerning the properties of the compound generator in various transient states, among other things, [4], [5], [13], and [14] and since the excitation scheme under consideration does not essentially differ from this in its nature, no closer study of transient phenomena is made in this paper.

7 PARALLEL OPERATION

The active power sharing between parallel generators is determined by the regulators of the prime movers. The active power sharing is therefore a problem independent of the characteristics of the generator and it is not considered here. On the other hand the reactive power sharing between parallel generators is determined by the characteristics of the generators and their regulators.

Consider two generators equipped with the excitation scheme under examination. The generators are loaded with a common passive load $Z\underline{/\varphi}$. Denote one of the generators by the subscript a and the other by the subscript b. As a consequence of the parallel connection,

$$U_a = U_b = U_1 \tag{143}$$

$$I_a = I_{aa} + I_{ba} = \frac{U_1 \cos\varphi}{Z} \tag{144}$$

$$I_r = I_{ar} + I_{br} = \frac{U_1 \sin\varphi}{Z} \tag{145}$$

Further, the active power sharing, i.e. the ratio of the active powers ($\overline{p}$), is determined by the regulators of the prime movers:

$$\overline{p} = \frac{P_a}{P_b} = \frac{I_{aa}}{I_{ba}} \tag{146}$$

Denote the unknown ratio of the reactive powers by $\overline{l}$

$$\overline{l} = \frac{Q_a}{Q_b} = \frac{I_{ar}}{I_{br}} \tag{147}$$

From Eqs. (144), (145), (146), and (147) the load of generator a is obtained:

$$Z_a = \frac{U_1}{\sqrt{I_{aa}^2 + I_{ar}^2}} = \frac{Z}{\sqrt{\left(\frac{\overline{p}}{1+\overline{p}}\right)^2 \cos^2\varphi + \left(\frac{\overline{l}}{1+\overline{l}}\right)^2 \sin^2\varphi}} \tag{148}$$

$$\varphi_a = \arctan\frac{I_{ar}}{I_{aa}} = \arctan\left(\frac{\overline{l}}{\overline{p}}\,\frac{1+\overline{p}}{1+\overline{l}}\tan\varphi\right) \tag{149}$$

and the load of generator b:

$$Z_b = \frac{U_1}{\sqrt{I_{ba}^2 + I_{br}^2}} = \frac{Z}{\sqrt{\left(\frac{1}{1+\overline{p}}\right)^2 \cos^2\varphi + \left(\frac{1}{1+\overline{l}}\right)^2 \sin^2\varphi}} \tag{150}$$

$$\varphi_b = \arctan \frac{I_{br}}{I_{ba}} = \arctan \left(\frac{1 + \bar{p}}{1 + \bar{I}} \tan \varphi \right) \tag{151}$$

In addition to the reactive power supplied to the load, a transfer of reactive power may occur between the generators. The reactive powers of the generators are determined so that the terminal voltages are equal. The reactive power sharing can be calculated by iterating $\bar{I}$ (147) to make the terminal voltage of generator a when used as an isolated generator on the load (148), (149) equal to that of generator b when used as an isolated generator on the load (150), (151). Next, the reactive currents can be resolved from the set of equations (145), (147).

The magnitude of the reactive currents depends on the saturation characteristics of the generators. Sufficiently accurate designing of the saturation characteristics is a highly difficult problem in practice. It follows that generators with the excitation scheme under consideration cannot be driven in parallel when negatively compounded. The same is true for conventional compounded generators. However, parallel operation of conventional compounded generators is possible e.g. by connecting the field windings in parallel and supplying them from a common compound exciter. Then, the generators being identical, the field currents are equal and no current will circulate in the machines. This scheme can also be used with generators of different size if the resistances of the field windings are properly dimensioned.

In the excitation scheme under investigation the field windings cannot be connected in parallel if the generators are not provided with brushgear. The absence of such gear is precisely an advantage of the system.

Parallel operation is possible by connecting one of the generators to be negatively compounded and the others to be positively compounded. The negatively compounded machine constitutes an "infinite bus" and supplies the reactive power required. The positively compounded generators supply mainly the active power and operate with a constant power factor. Similarly, parallel operation of the excitation scheme under consideration on an infinite bus is only possible with positive compounding.

8 EXPERIMENTAL INVESTIGATIONS

8.1 EXPERIMENTAL GENERATOR

For testing the harmonic excitation scheme under consideration an experimental generator, designed as follows, was built.

Rating: 3 kVA, 3-phase 280 V, Y-connected, 6,1 A, 50 Hz, 1500 r/min. The generator had no fan, and the windings were not impregnated in view of easier changes. Therefore the nominal load could not be determined by a temperature-rise test. The rating of a salient-pole generator with identical outer dimensions of the lamination was taken to represent the nominal load.

Stator: length 103 mm, effective length L = 104,5 mm, outer diameter = 235 mm, air-gap diameter D = 180 mm, air-gap length δ = 0,74 mm, number of slots Q_1 = 30, number of poles $2p$ = 4, slots per pole per phase q_1 = 2,5, stator winding as shown in Fig. 6, single-layer fractional-slot winding, chorded on the average 7/7,5, number of conductors per slot N_{1u} = 26, number of turns in series per phase N_{1t} = 130, diameter of conductor = 1,4 mm, material copper, winding factor for the fundamental ξ_{1p} = 0,952, slot-opening factor (18) for 16th harmonic (slot harmonic) $\xi_{\epsilon(p+Q1)}$ = 0,953. The stator slot dimensions are seen in Fig. 37. To enable the relation between the two components of the field current to be changed, the stator slot opening was dimensioned in excess of what is correct on the basis of the relation of the field current components; partly magnetic and partly non-magnetic slot wedges were employed. The magnetic slot wedges were made of lengths of iron wire 0,5 mm thick, which were molded in resin to make a wedge. The density of these wedges was found by measurement to be 5,2 kg/dm^3. Adequate voltage characteristics were obtained when the magnetic slot wedges had a length of 47 mm. All measurements reported below are valid for this length of the magnetic wedges unless otherwise stated.

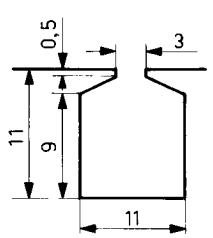

Fig. 37. Stator slot dimensions of the experimental generator (in millimetres).

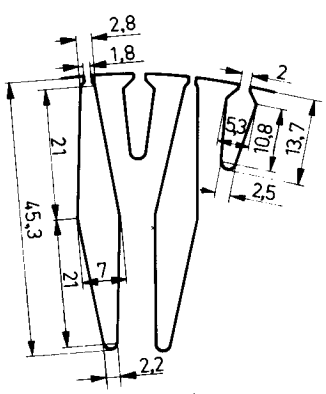

Fig. 38. Rotor slot dimensions of the experimental generator (in millimetres).

Rotor: non-salient-pole rotor, length = 103 mm, air-gap diameter = 178,5 mm. *Field winding:* number of slots = 32, coiled slots = 24, number of conductors per slot = 130, number of turns in series N_{Ft} = 1560, all poles connected in series, diameter of conductors = 0,85 mm, material copper, winding placed on the bottom of the slot, winding factor for the fundamental ξ_{Fp} = 0,790, reduction factor μ = 0,213; the rotor slot dimensions are seen in Fig. 38. *Auxiliary winding:* The winding supplying the field winding was made for the first slot harmonic rotating in the same direction as the fundamental. The winding was a one-phase full-pitch winding, number of slots = 64, every second slot being the upper part of the field winding slot and the rest being the smaller slots between the greater slots of the field winding (Fig. 38); number of poles = 64, number of slots per pole per phase = 1, number of conductors per slot N_{Au} = 33, number of turns in series N_{At} = 1056, diameter of conductor = 0,85 mm, material copper, winding factor $\xi_{A,32}$ = 1,0.

For the measurements, the generator was fitted with two pairs of slip rings, one for the field winding and the other for the auxiliary winding.

The no-load magnetization and short-circuit characteristics and the induced voltage in the auxiliary winding at no-load are shown in Fig. 39. The generator was separately excited in all instances. The measurements were made with and without magnetic slot wedges. The magnetic wedges did not influence the magnetization nor the short-circuit curves within the accuracy of measurement. On the contrary, they had an effect on the induced voltage of the auxiliary winding.

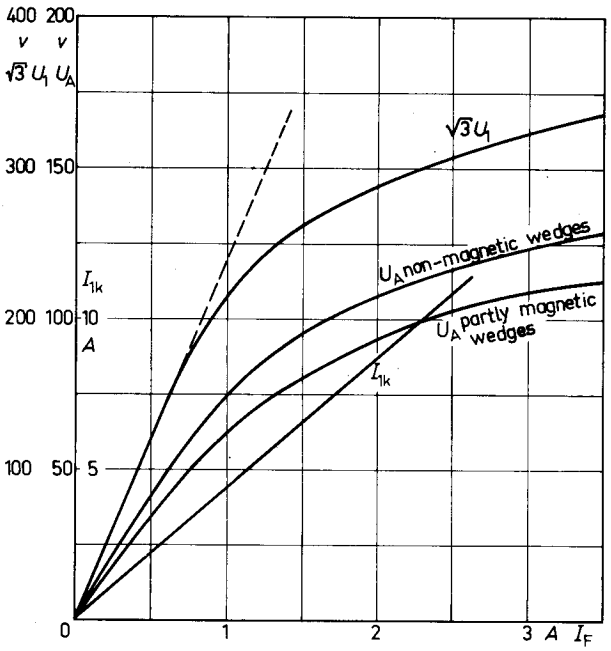

Fig. 39. The experimental generator's magnetization curve ($\sqrt{3}\,U_1$, stator line voltage), short-circuit curve (I_{1k}) and voltage induced in the auxiliary winding (U_A) at no-load.

Carter's coefficient is, according to RICHTER [19, p. 173], $k_c = 1{,}16$. The value is calculated without magnetic wedges. Carter's coefficient with the magnetic wedges can be calculated as set forth in [11]. In this case the influence of the wedges on Carter's coefficient was small, seeing that the open-circuit curves were equal with and without magnetic wedges. For this reason the value 1,16 obtained above is used for Carter's coefficient in the following calculations.

8.2 CIRCUIT ELEMENTS

8.2.1 Resistances

The temperature of the windings averaged 50°C in the measurements. The resistances in direct current corrected to this temperature are: resistance of the stator phase winding $R_1 = 1{,}11\,\Omega$, resistance of the field winding $R_F = 22{,}4\,\Omega$, and resistance of the auxiliary winding $R_A = 12{,}6\,\Omega$. The frequency in the auxiliary winding is 750 Hz. The ratio of the effective resistance to d.c. resistance is found according to [19, p. 245] to be 1,07. In the calculations the value $R_A = 1{,}07 \cdot 12{,}6\,\Omega = 13{,}5\,\Omega$ shall be used for the resistance of the auxiliary winding.

8.2.2 Reactances

Leakage reactance of stator winding. In the calculation of the terminal voltage it is assumed in Eqs. (124) ··· (126) that the rotor is not saturated by its leakage flux. The error incurred may be partly eliminated by using, instead of the stator leakage reactance, the so-called Potier reactance. A Potier reactance of $2{,}0\,\Omega$ was measured by Fisher-Hinnen's method [22] at the rated voltage (280 V).

Reactance of auxiliary winding. The sum of the magnetizing and harmonic leakage reactances can be calculated by the aid of the magnetic field energy generated by the winding in the air-gap. The distribution of the field strength produced in the air-gap by a current i is shown in Fig. 40. The magnetic field energy in the equivalent air-gap δ_ν'' is

$$W = \frac{Q_A}{2}\,\mu_0 h^2 \tau_A L \delta_\nu'' = \frac{\pi}{8}\,\frac{\mu_0}{\delta_\nu''}\,DL N_{Au}^2 i^2 \tag{152}$$

whence the sum of the magnetizing and harmonic leakage reactances X_{Am} is obtained:

$$X_{Am} = \frac{2\omega_\nu W}{i^2} = \frac{\pi}{4}\,\frac{\mu_0}{\delta_\nu''}\,\omega_\nu DL N_{Au}^2 \tag{153}$$

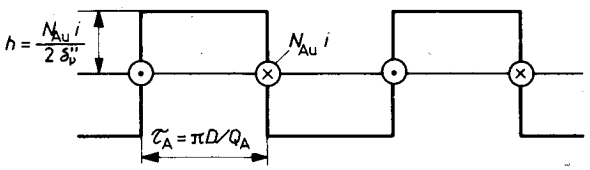

Fig. 40. The magnetic field strength in the air-gap produced by a current i flowing in the auxiliary winding.

The unsaturated value of X_{Am} is obtained when $\delta_\nu'' = k_c\delta$. Substituting the values of the experimental generator, we have

$$X_{Am} = 110\,\Omega$$

The slot leakage reactance of the auxiliary winding is calculated according to [19, p. 268] $X_{Au} = 78{,}9\,\Omega$, the tooth-top leakage reactance [20, p. 90] $X_{Az} = 12{,}8\,\Omega$, and the end-winding leakage reactance [20, p. 91] $X_{Ay} = 4{,}3\,\Omega$ (length of the end-winding = 70 mm). The leakage reactance and the synchronous reactance of the auxiliary winding are

$$X_{A\sigma} = X_{Au} + X_{Az} + X_{Ay} = 96{,}0\,\Omega$$

$$X_A = X_{Am} + X_{A\sigma} = 206\,\Omega$$

Results of measurement. The synchronous reactance of the auxiliary winding can be determined from the equation

$$X_A = \sqrt{\left(\frac{U_A}{I_{Ak}}\right)^2 - R_A^2}$$

where U_A is the terminal voltage at no-load and I_{Ak} the short-circuit current of the auxiliary winding when the generator is separately excited. U_A and I_{Ak} were measured as a function of the stator current with load power factors zero lagging, and unity. The field current was regulated to maintain a constant air-gap voltage U_i. For determing U_i, a search coil was attached to the air-gap surface.

The reactance measured as a function of the field current, with U_i and the power factor as parameters, is shown in Fig. 41. The point on each curve (except on the curve for $U_i = 0$) measured with the smallest field current corresponds to the no-load condition, i.e. to $I_1 = 0$. When $U_i = 0$, the stator winding was three-phase short-circuited.

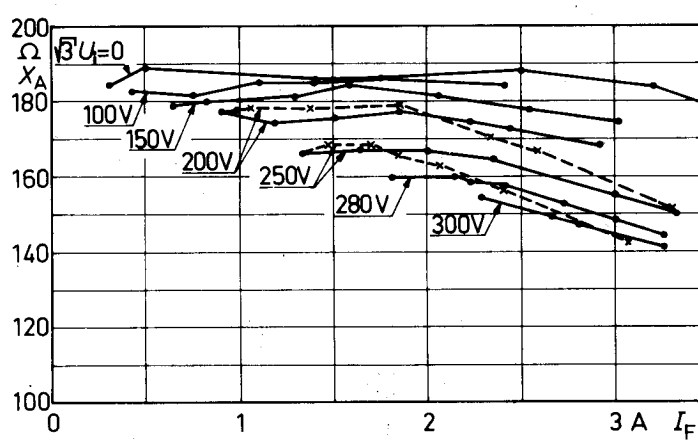

Fig. 41. Measured reactance (X_A) of the auxiliary winding *vs.* field current (I_F), with air-gap voltage (U_i) and power factor ($\cos\varphi$) as parameters. ⟶ $\cos\varphi = 0$ lag, –x– –x– $\cos\varphi = 1$.

As seen from Fig. 41, X_A is constant when U_i and the power factor are constant and $I_F < 1{,}7 \cdots 2$ A. When the load current is high enough to make $I_F > 1{,}7 \cdots 2$ A, X_A begins to decrease. It follows that when $I_F < 1{,}7 \cdots 2$ A and when the resulting flux is constant (i.e., U_i is constant) the equivalent air-gap δ''_ν is constant for the first slot harmonic. When the field current exceeds the limiting point, the leakage flux of the rotor begins to saturate the rotor teeth and δ''_ν increases, causing X_A to decrease. Fig. 42 shows schematically the leakage flux pattern of the rotor. The saturation caused by the leakage flux is strongest in the tooth denoted with A.

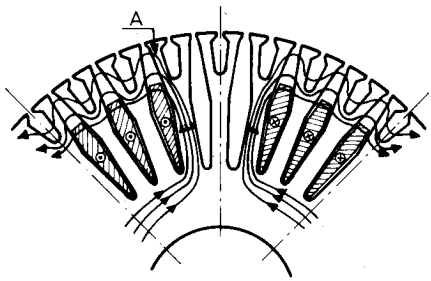

Fig. 42. The leakage flux of the rotor. The tooth A is most strongly saturate.

As can be seen from Fig. 41, the reactance of the auxiliary winding decreases when the resulting flux increases (when U_i increases). This is due to the saturation of the rotor teeth, especially at the maximum of the air-gap flux density. Because the saturation of the teeth varies along the rotor surface, the saturation is difficult to calculate. In addition, the saturation depends on the phase of the load current as can also be seen from Fig. 41. The inverse value of the equivalent air-gap of the first slot harmonic and the magnetizing reactance at no-load conform approximately to the formula

$$\frac{k_c \delta}{\delta''_\nu} = \frac{X_{Am}}{X_{Am,\,unsat}} = \frac{\hat{v}_\delta}{\hat{v}_\delta + \hat{v}_{z2}}$$

where $\hat{v}_{z2}$ is the tooth m.m.f. of the rotor and $\hat{v}_\delta$ the m.m.f. of the air-gap $k_c\delta$ at the centre of the pole, and $X_{Am,\,unsat}$ is the unsaturated value of X_{Am}.

According to Fig. 41 the unsaturated value of X_A ($U_i \approx 0$) is about 185 Ω. The calculated value was 206 Ω, that is, slightly higher. Assuming that the calculated leakage reactance $X_{A\sigma} = 96\ \Omega$ is correct, the unsaturated magnetizing reactance is found to be $X_{Am,\,unsat} = 89\ \Omega$.

The ratio $X_{Am}/89\ \Omega$ calculated from the results of measurement is displayed as a function of the no-load field current in Fig. 43. The function $\hat{v}_\delta/(\hat{v}_\delta + \hat{v}_{z2})$ computed according to RICHTER [19], [20] in terms of the no-load field current has been entered in the same diagram. The functions $X_{Am}/89\ \Omega$ and $\hat{v}_\delta/(\hat{v}_\delta + \hat{v}_{z2})$ have a similar character. However, $\hat{v}_\delta/(\hat{v}_\delta + \hat{v}_{z2})$ shows a somewhat stronger dependence on the saturation than $X_{Am}/89\ \Omega$.

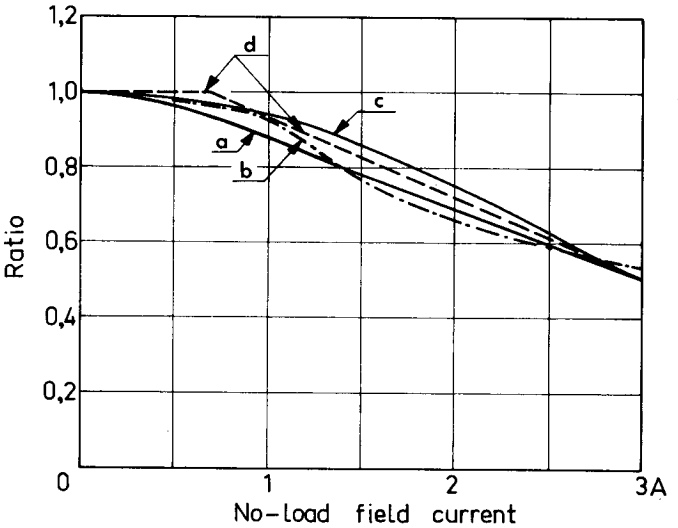

Fig. 43. a) The ratio of the magnetizing reactance X_{Am} of the auxiliary winding to the value 89 Ω calculated from results of measurement, b) the ratio $\hat{v}_\delta/(\hat{v}_\delta+\hat{v}_{z2})$, c) the ratio $C_2/15{,}7\ \frac{V}{A}$ calculated from results of measurement, and d) the function $k_c\delta/\delta''_v$ used in calculating the terminal voltage. All ratios presented as functions of the no-load field current.

8.2.3 Factor C_1

From Fig. 15 we obtain, without magnetic slot wedges, $\hat{\Lambda}_{Q1}/\Lambda_0 = 0{,}16$ when $x_{41}/t_1 = 0{,}16$ and $x_{41}/\delta = 4{,}05$. Further, according to Eq. (108), $C_1 = 0{,}58$.

The factor C_1 is according to Eq. (107) the ratio of the induced voltage of the auxiliary winding to the induced voltage of the stator winding at no-load when the generator is separately excited. Fig. 44 shows the measured terminal voltage (U_A) of the auxiliary winding as a function of the stator line voltage ($\sqrt{3}\,U_1$) at no-load and at rated speed, with and without magnetic slot wedges. As can be seen from the figure, the relation between U_A and U_1 is linear over a wide range. When U_1 exceeds $230/\sqrt{3}$ V, the voltage of the auxiliary winding increases at a rate faster than linear and C_1 increases. With magnetic slot wedges this non-linearity is slightly stronger than with non-magnetic wedges. Obviously the magnetic wedges are saturated to a certain degree, causing an apparent increase of the slot opening.

From Fig. 44 we obtain, in the range $U_1 = 0 \cdots 230/\sqrt{3}$ V without magnetic slot wedges,

$$C_1 = \frac{U_A}{U_1} = 0{,}62$$

which is slightly in excess of the calculated value. With magnetic wedges we obtain from Fig. 44, $C_1 = 0{,}49$ in the range $U_1 = 0 \cdots 230/\sqrt{3}$ V, and at the rated voltage $U_1 = 280/\sqrt{3}$ V we have $C_1 = 0{,}55$.

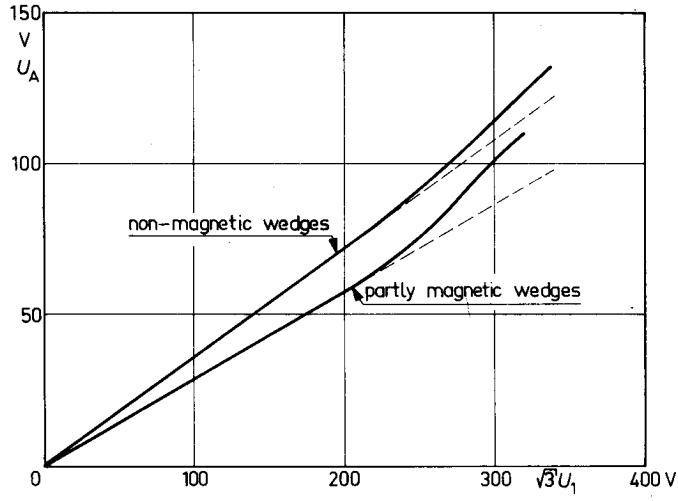

Fig. 44. Measured voltage (U_A) of the auxiliary winding *vs.* stator line voltage ($\sqrt{3}\ U_1$) at no-load; separate excitation.

8.2.4 Factor C_2

The factor C_2 is, according to Eq. (111), a function of the saturation (δ''_v). The unsaturated value is obtained from Eq. (111) with air-gap $k_c\delta$:

$$C_2 = 15{,}1\ \text{V/A}$$

According to Eq. (110) C_2 is the ratio of the voltage component U_{Afk} of the auxiliary winding induced by the stator current and of the stator current I_1. The measured voltage of the auxiliary winding, as a function of the stator current, is displayed in Fig. 45 at a load power factor of zero lagging. The field current was regulated to maintain a constant air-gap voltage U_i. The measurements were performed with several values of U_i. C_2 is the slope of the tangent of the family of curves obtained, because at zero p.f. lag the voltage components induced in the auxiliary winding, of which one is proportional to U_i and the other is proportional to I_1, are in phase, and with a constant U_i the stator current I_1 alone causes a change of the voltage of the auxiliary winding. As can be seen from Fig. 45, the function $U_{Afk} = f(I_1)$ is at small voltages ($U_i \approx 0 \cdots 150/\sqrt{3}$ V) linear, independent of the load current. Within this range C_2 depends only on the voltage. At higher voltages ($U_i > 150/\sqrt{3}$ V) the relation $U_{Afk} = f(I_1)$ is linear with small currents, becoming non-linear for higher currents. At the limiting point the field current is about 2 A, at which current the magnetizing reactance X_{Am} was also found to become saturated owing to the rotor leakage flux. The unsaturated value of C_2 is found from the measurements at small voltages to be $C_2 = 15{,}7$ V/A, which is slightly higher than calculated (15,1 V/A).

Fig. 43 shows $C_2/15{,}7$ V/A calculated from the initial slopes of the measured curves, as a function of the no-load field current. The function thus obtained is similar to X_{Am} and to $\hat{v}_\delta/(\hat{v}_\delta + \hat{v}_{z2})$. This is exactly as should be, since they are all proportional to $1/\delta''_v$.

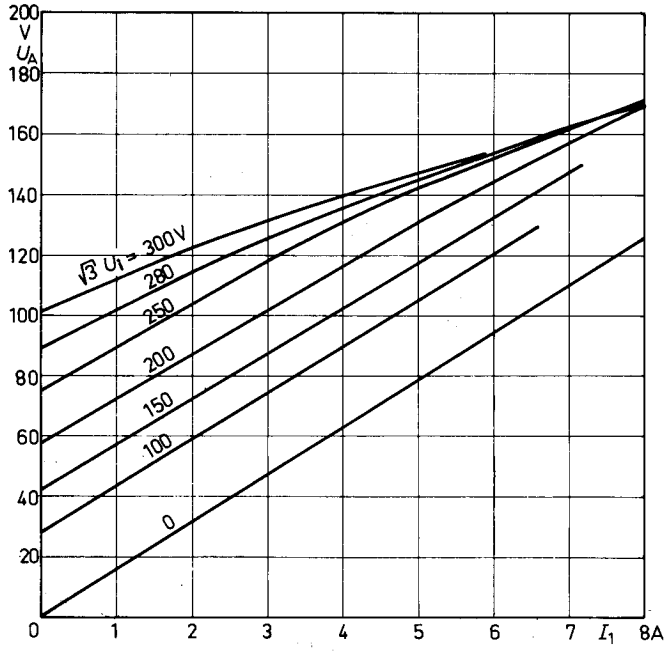

Fig. 45. Measured terminal voltage (U_A) of the auxiliary winding *vs.* stator current (I_1), with air-gap voltage ($\sqrt{3}\ U_i$) as parameter. The load power factor is zero lagging and the generator is separately excited.

8.3 TERMINAL VOLTAGE

8.3.1 Terminal voltage as a function of load current

The terminal voltage of the generator as a function of the load current at various power factors is shown in Fig. 46, the generator being separately excited with a constant current.

The measurements with self-excited mode were performed using the capacitors $C = 1{,}70\ \mu F$ and $C_k = 0{,}98\ \mu F$. C_k was chosen to ensure a safe build-up. The nominal operating point was within the range where a small decrease of the speed had little influence on the terminal voltage. The rectifier and capacitors were mounted on the rotor, so that the slip rings would not interfere with the measurements. The measured load characteristics and those calculated according to Chapter 6.4 at three different power factors are shown in Fig. 47. In the calculations $k_c\delta/\delta''_\nu$ was assumed to conform to the two straight lines drawn in Fig. 43, which present a satisfactory fit with the measured X_{Am} and C_2 curves. Instead of the no-load field current, the resulting field current I_ϕ corresponding to the internal operating point was used in the calculations. I_ϕ determines the saturation state at load. The increasing saturation due to the rotor leakage flux at higher load currents was not taken into account. The value $C_2 = 15{,}7$ V/A was used for non-saturation C_2, the value $X_{Am,\,unsat} = 89\ \Omega$ for non-saturation X_{Am}

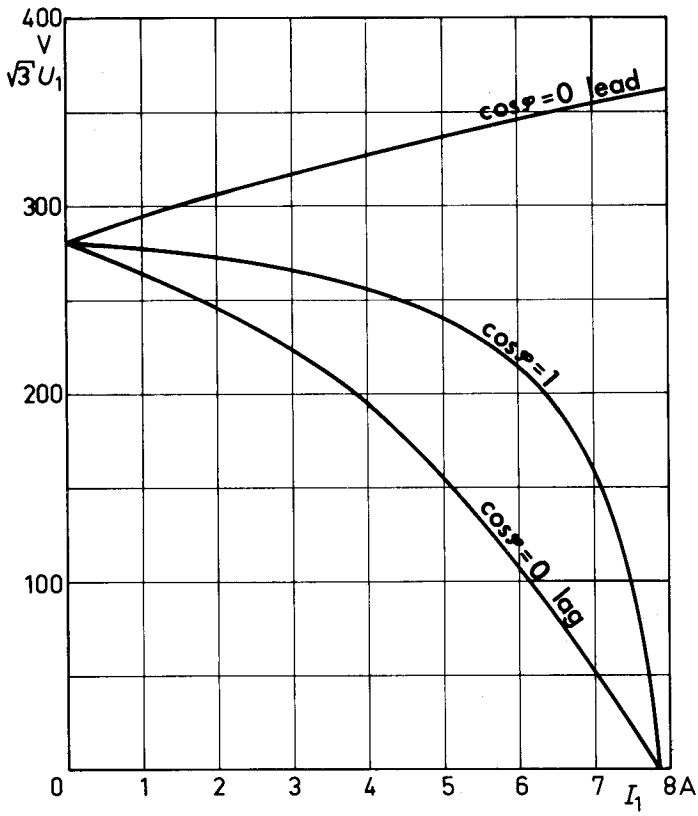

Fig. 46. The measured load characteristics of the experimental generator when excited separately by a constant field current.

and the value $X_A = 96\ \Omega$ for the leakage reactance. A constant value $C_1 = 0{,}55$ measured at the rated voltage was used for the factor C_1.

According to the measurements as well as the calculations the voltage of the generator remains satisfactorily constant within the range $I_1 = 0 \cdots I_{1N}$(I_{1N} = rated current), except at zero p.f. lead. At lagging power factors the deviation from the rated voltage is $+3{,}6\,\% \cdots -1{,}8\,\%$. At zero p.f. lead the voltage declines to zero at a load current about $I_1 = 4$ A, but the voltage once again builds up when the capacitor load is augmented. A similar characteristic is also obtained by calculation. It is true, though that the calculated voltage did not become zero at $I_1 = 4$ A. This is due to the fact that the calculating method does not satisfactorily account for the great changes of saturation occurring in the case under consideration when the voltage decreases strongly. When the load current is in excess of the rated current, the terminal voltage begins to fall at unity p.f. and at lagging power factors. In this range the calculated curves differ considerably from the measured curves. This is because in this range the saturation of X_{Am} and of C_2 also depend on the load current, as has been observed previously, and this phenomenon is not taken into account in the calculations.

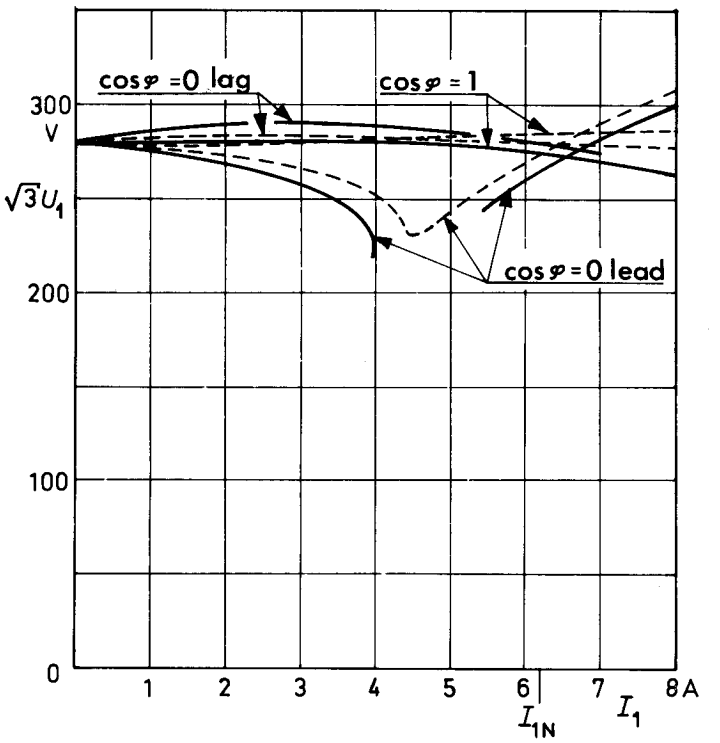

Fig. 47. Load characteristics of the experimental generator when self-excited; ——— measured, ----- calculated. I_{1N} = rated current.

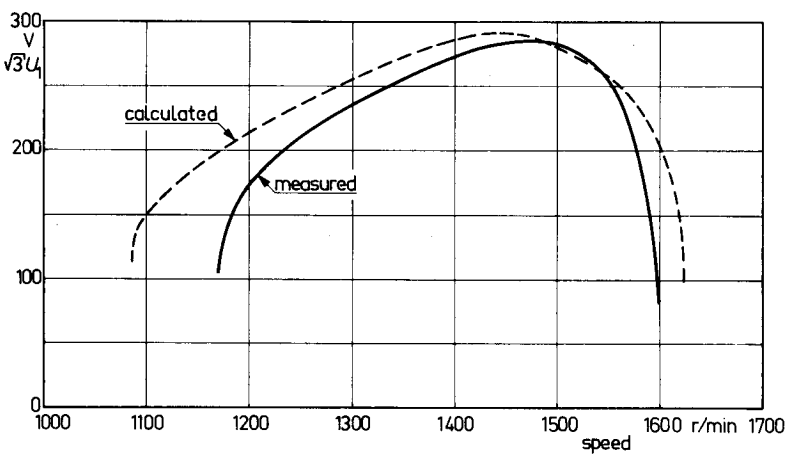

Fig. 48. No-load line voltage of the experimental generator *vs.* speed.

8.3.2 Terminal voltage as a function of speed

The measured terminal voltage of the generator, as a function of the speed at no-load, is shown in Fig. 48, the generator being self-excited. The characteristic has a nature qualitatively like that obtained in Chapter 6.5. Fig. 48 also contains the same characteristic calculated according to the diagram of Fig. 34 ($Z_L = \infty$). The constants and the function $k_c\delta/\delta''_\nu$ used in the calculations are the same as in the preceding chapter. The calculated curve shows a satisfactory fit with the measured curve.

8.3.3 Sudden load change

The oscillograms in Fig. 49 reveal the behaviour of the generator when the rated inductive current (6,2 A, p.f. zero) is suddenly connected and disconnected. With a pure inductive load the change of the field current is greatest. The change of the speed is small, because the change of the active power is nearly zero. The terminal voltage initially falls by the amount of the voltage drop in the transient reactance. After the sudden change, the voltage begins to rise and aperiodically reaches the steady-state value; the time for recovery to within 2,5 % of the rated voltage is about 0,2 s. The alternating component induced in the field winding by the d.c. component of the stator current is observable in the field voltage. When current is supplied to the load, the field voltage mean suddenly changes by an amount equalling the excitation voltage component proportional to the load current. On disconnection of the load the transient phenomena are similar, but reversed. The recordings resemble the corresponding oscillograms of a conventional compounded generator [14].

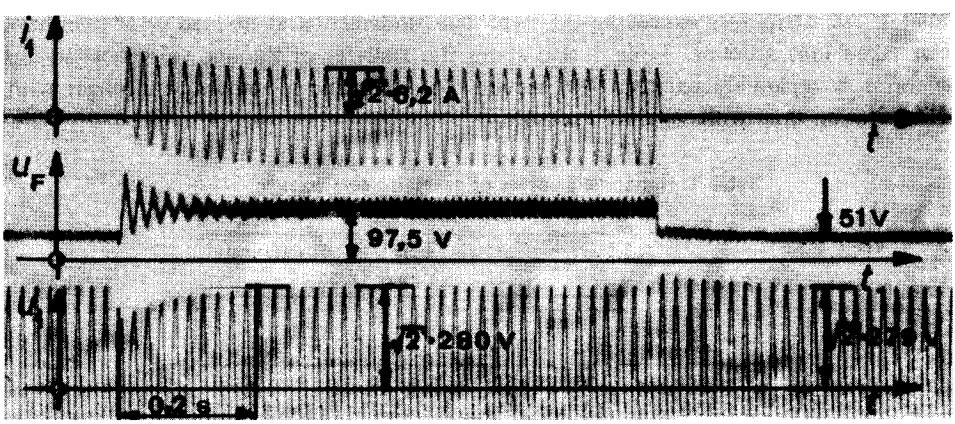

Fig. 49. The stator current (i_1), field voltage (u_F) and stator line voltage (u_1) when an inductive load (I_1 = 6,2 A, p.f. zero lagging) is connected and disconnected. The generator is self-excited.

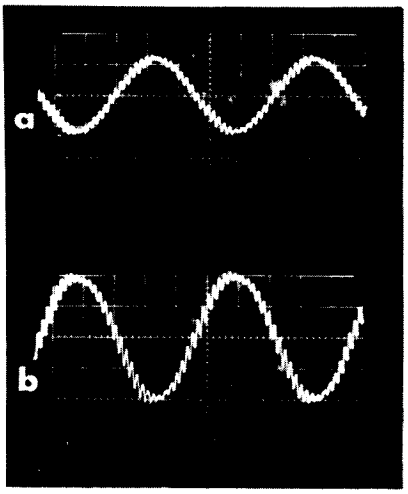

Fig. 50. The stator terminal voltage at no-load when the generator is self-excited; a) voltage to neutral, b) line voltage.

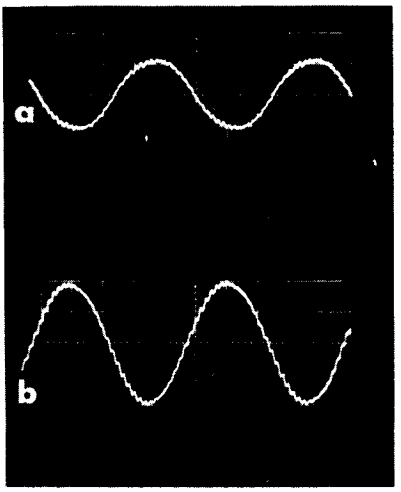

Fig. 51. The stator terminal voltage when the generator is self-excited and loaded by the rated current (6,2 A) at unity power factor; a) voltage to neutral, b) line voltage.

8.3.4 Terminal voltage waveform

The waveform of the terminal voltage of the generator at no-load is shown in Fig. 50 when the generator is self-excited. In Fig. 51 the corresponding curves are shown when the generator supplies the rated current at unity power factor. As can be seen from the figures, a strong second slot harmonic is induced in the terminal voltage. It is suppressed to some degree at load. The harmonic analyses of the line voltages are represented in Table 1. All harmonics exceeding 0,5 % of the fundamental at no-load or at load have been taken into account. Table 1 also states the analyses of the line voltage when the generator is separately excited. The second slot harmonic is somewhat stronger with self-excitation than with separate excitation.

Table 1. Harmonic analyses of generator line voltage. a. Self-excitation b. Separate excitation

Frequency Hz	No-load		Full load current, unity power factor	
	a %	b %	a %	b %
50	100	100	100	100
150	1,3	0,8	1,0	1,5
250	1,0	1,0	0,6	0,5
350	-	0,1	0,6	0,5
1450	9,4	7,1	2,7	1,6
1550	7,1	3,6	1,9	1,5
2950	0,6	0,4	-	-
3050	0,1	0,5	-	-

9 CONCLUSIONS

It has been shown that it is possible to construct a brushless self-regulated synchronous generator excited by harmonics of the flux density distribution. The field current component proportional to the resulting flux can only be produced by permeance variations due to irregularities of the stator's air-gap face. The field current component proportional to the load current can be produced by harmonics due to the stator winding distribution. The first slot harmonic is most useful in that with its aid the highest field current is obtained, and it is possible to make the number of damper-bars equal to that in conventional generators. A drawback of the first slot harmonic is the great number of poles, whereby it may become more difficult to make the auxiliary winding for the slot harmonic than for a lower harmonic. Moreover, fewer methods are available for elimination of harmonics from the stator terminal voltage in the case of slot harmonics than in that of lower harmonics.

The stator terminal voltage depends on the saturation of the generator. The measurements performed with an experimental generator show that the method presented for calculating the terminal voltage gives a satisfactory result in practice.

Parallel operation on an infinite bus is possible with positive compounding, in which case the generator acts at a constant power factor. Several generators with harmonic excitation can be connected in parallel if one of the generators is negatively compounded and supplies the required reactive power, while the other generators are positively compounded.

Manuscript received 1973–06–26

ACKNOWLEDGEMENTS

The work involved in this study was carried out at the Electromechanical Laboratory, Helsinki University of Technology. I wish to express my sincere gratitude to Professor Tauno Pyökäri for his interest in this work and for important discussions and advice. I also wish to thank the personnel of the laboratory for their support during this work, and my thanks are due to Mr. Uljas Attila, who revised the English text of the manuscript.

The financial support granted by Tekniikan Edistämissäätiö (Foundation of Technology) is acknowledged with gratitude.

REFERENCES

1. BIGGS, F.I. and NIPPES, P.I., Harmonic excitation of synchronous machines. Proc. Amer. Power Conf. 23(1961), pp. 900 ··· 907.

2. BOLLER, H.W. and JORDAN, H., Über die phasenrichtige Addition der nutharmonischen Wicklungsoberfelder und Nutungsoberfelder bei phasenreinen Mehrphasenwicklungen. Elektrotech. Z. Ausg. A 84(1963)7, pp. 235 ··· 238.

3. BÖDEFELD, Th. and SEQUENZ, H., Elektrische Maschinen. 8th ed. Wien, Springer-Verlag, 1971. 813 p.

4. BÖSKEN, H., Untersuchung über das statische und dynamische Verhalten von Kompoundierungsschaltungen mit Zusatzregelung. Diss., Technische Hochschule Braunschweig, 1965. 171 p.

5. DROSTE, W., Die Untersuchung des statischen und dynamischen Verhaltens von kompoundierten Synchronmaschinen in Stromzwangschaltung. Diss., Technische Hochschule Darmstadt, 1964. 115 p.

6. FREEMAN, E.M., The calculation of harmonics, due to slotting, in the flux density waveform of a dynamo-electric machine. Proc. Inst. Elec. Eng., Part C 109(1962)16, pp. 581 ··· 588.

7. FREJTICH, Z. and SIEGL, M., Harmonische der Leitfähigkeit einseitig genuteter Luftspalte elektrischer Maschinen. Acta Tech. ČSAV (1970)2, pp. 164 ··· 174.

8. FROHNE, H., Über die primären Bestimmungsgrössen der Lautstärke bei Asynchronmaschinen. Diss., Technische Hochschule Hannover, 1959. 194 p.

9. JORDAN, H., Der geräuscharme Elektromotor. Essen, Girardet, 1950. 97 p.

10. KEHSE, W., Beitrag zur Kenntnis der Feldverteilung im Luftspalt der Asynchronmaschine. Diss., Technische Hochschule Darmstadt, 1938. 59 p.

11. KUBRYCHT, J., Carter's coefficient of a slot with a magnetic wedge. Acta Tech. ČSAV (1971)6, pp. 693 ··· 703.

12. LEHMAN, S., Über die Kraftwellen-Ordnungszahlenschemata für die rechnerische Untersuchung magnetischer Geräusche an Drehstrommaschinen und die Ermittlung mittels elektronischer Digital-Rechenautomaten. Diss., Technische Hochschule Darmstadt, 1961. 137 p.

13. LUBASCH, R., Zeitlicher Verlauf der Systemgrössen von kompoundierten Synchronmaschinen bei Stosskurzschluss. Diss., Technische Hochschule Karlsruhe 1969. 99 p.

14. LUTZ, K., Konstantspannungs-Synchrongeneratoren. Einteilung, Ausgleichsgeschwindigkeit, Spannungsgenauigkeit. Elektrotech. Maschinenbau 78(1961)3, pp. 144 ··· 151.

15. NIPPES, P.I., Harmonic power in nonsalient-pole synchronous machinery. Trans. Amer. Inst. Elec. Eng., Part III 81(1962)62, pp. 419 ··· 424.

16. NORMAN, H., Induction motor locked saturation curves. Elec. Eng. 53(1934)4, pp. 536 ··· 541.

17. PLATTHAUS, L., Selbsterregung von Synchronmaschinen durch die dritte Harmonische des Luftspaltfeldes. Diss., Technische Hochschule, Aachen 1964. 126 p.

18. PYÖKÄRI, T., Sähkökoneoppi (in Finnish). Helsinki, Sininen Kirja Oy, 1971. 485 p.

19. RICHTER, R., Elektrische Maschinen I. 2nd ed. Basel, Verlag Birkhäuser, 1951. 630 p.

20. RICHTER, R., Elektrische Maschinen II. 2nd ed. Basel, Verlag Birkhäuser, 1953. 707 p.

21. ROCHE, L.R., A harmonic excitation system for turbine generators. Trans. Amer. Inst. Elec. Eng., Part III 81(1962)60, pp. 105 ··· 109.

22. SCHUISKY, W., Kritische Betrachtung des Verfahrens zum Bestimmen der Lasterregung von Synchronmaschinen. Siemens-Z. 38(1964)5, pp. 365 ··· 369.

23. TÜXEN, E., Das Oberwellenverhalten mehrphasiger Wechselstromwicklungen. Jahrb. AEG-Forsch. 8(1941)2, pp. 78 ··· 105.

24. VOLKMANN, W., Übersicht über Kompoundierungsschaltungen für Synchrongeneratoren. Elektrotech. Z. Ausg. A 81(1960)26, pp. 932 ··· 937.

25. WEBER, E., Der Nutungsfaktor in elektrischen Maschinen. Elektrotech. Z. 49(1928)23, pp. 858 ··· 861.

26. v. ZWEYGBERGK, S., Teorin för kortslutningsmotor med trefas-delspår-övergångslindning. (The theory of squirrel-cage motor with three-phase fractional-slot double-layer winding, in Swedish.) Diss., Helsinki University of Technology, 1949. 139 p.

ISBN 951–666–024–X

VTT OFFSETPAINO 1973
495/1